JEM Journal of Experimental Medicine

ARTICLE

Targeting leukocidin-mediated immune evasion protects mice from *Staphylococcus aureus* bacteremia

Kayan Tam[1], Keenan A. Lacey[1], Joseph C. Devlin[1], Maryaline Coffre[2], Alexis Sommerfield[1], Rita Chan[1], Aidan O'Malley[1], Sergei B. Koralov[2], P'ng Loke[1,3], and Victor J. Torres[1]

Staphylococcus aureus is responsible for various diseases in humans, and recurrent infections are commonly observed. _S. aureus_ produces an array of bicomponent pore-forming toxins that target and kill leukocytes, known collectively as the leukocidins. The contribution of these leukocidins to impair the development of anti–_S. aureus_ adaptive immunity and facilitate reinfection is unclear. Using a murine model of recurrent bacteremia, we demonstrate that infection with a leukocidin mutant results in increased levels of anti–_S. aureus_ antibodies compared with mice infected with the WT parental strain, indicating that leukocidins negatively impact the generation of anti–_S. aureus_ antibodies in vivo. We hypothesized that neutralizing leukocidin-mediated immune subversion by vaccination may shift this host-pathogen interaction in favor of the host. Leukocidin-immunized mice produce potent leukocidin-neutralizing antibodies and robust Th1 and Th17 responses, which collectively protect against bloodstream infections. Altogether, these results demonstrate that blocking leukocidin-mediated immune evasion can promote host protection against _S. aureus_ bloodstream infection.

Introduction

Staphylococcus aureus is a gram-positive bacterium that can cause a range of diseases, from mild skin and soft-tissue infections to life-threatening conditions such as bacteremia (Tong et al., 2015; Wertheim et al., 2005). *S. aureus* is among the most common causes of bloodstream infections (BSIs), with a 30-d mortality rate of 20% (van Hal et al., 2012). Standard treatments for *S. aureus* infections include active prevention (i.e., decolonization of confirmed carriers) and rigorous antibiotic treatment upon infection (Gold and Pillai, 2009; Septimus and Schweizer, 2016). The latter approach contributes to the rise of multidrug-resistant *S. aureus* (Chambers and Deleo, 2009). An anti–*S. aureus* vaccine may offer a potential solution to this epidemic of antimicrobial resistance. However, identifying relevant antigens for vaccine development has proven to be challenging (Bagnoli et al., 2012; Giersing et al., 2016). To date, there is no Food and Drug Administration–approved vaccine to combat *S. aureus* infections. As such, we posit that a better understanding of how *S. aureus* affects the development of host adaptive immunity during infection can help to identify potential vaccine targets.

S. aureus has evolved to counter host defense mechanisms by producing a myriad of immune evasion factors (Foster, 2005; Thammavongsa et al., 2015). These immune evasion strategies promote bacterial survival and may contribute to the high incidence of recurrent *S. aureus* infections (Chang et al., 2003; Creech et al., 2015; Miller et al., 2007). One such family of virulence factors is the bicomponent pore-forming toxins, also known as leukocidins (Alonzo and Torres, 2014; Spaan et al., 2017). Pathogenic strains of *S. aureus* that infect the human host can produce and secrete up to five of these leukocidins—LukED, the γ-hemolysins (HlgAB and HlgCB), Panton-Valentine leukocidin (also known as LukSF-PV), and LukAB (also known as LukGH; Alonzo and Torres, 2014; Spaan et al., 2017). Together, the leukocidins can target and kill a wide array of primary human leukocytes critical for innate immune defenses and adaptive immunity, including neutrophils, monocytes, macrophages, dendritic cells, and effector memory T cells (Alonzo et al., 2013; Alonzo and Torres, 2014; Berends et al., 2019; DuMont et al., 2011; Reyes-Robles et al., 2013; Spaan et al., 2013, 2015, 2017). While all the leukocidins have strong tropism toward human cells, LukED and HlgAB are also active toward murine cells, thus allowing us to study the effects of these leukocidins in vivo (Alonzo et al., 2013; Lubkin et al., 2019; Reyes-Robles et al., 2013; Spaan et al., 2015, 2014). We hypothesize that the leukocidins act as immune subversion molecules that interfere with the development of adaptive immunity during *S. aureus* infection. Therefore, neutralizing the activity of these immune evasion

[1]Department of Microbiology, New York University Grossman School of Medicine, New York, NY; [2]Department of Pathology, New York University Grossman School of Medicine, New York, NY; [3]Laboratory of Parasitic Diseases, National Institute of Allergy and Infectious Diseases, National Institutes of Health, Bethesda, MD.

Correspondence to Victor J. Torres: Victor.Torres@NYULangone.org.

© 2020 Tam et al. This article is distributed under the terms of an Attribution–Noncommercial–Share Alike–No Mirror Sites license for the first six months after the publication date (see http://www.rupress.org/terms/). After six months it is available under a Creative Commons License (Attribution–Noncommercial–Share Alike 4.0 International license, as described at https://creativecommons.org/licenses/by-nc-sa/4.0/).

molecules through vaccination can protect the host from *S. aureus* infection.

In this study, we investigated the role of the leukocidins LukED and HlgAB in interfering with the development of adaptive immunity during BSI in mice. Our findings establish that these leukocidins can blunt the generation of antibody responses against the bacterium. However, vaccination against the leukocidins can inhibit leukocidin-mediated immune subversion and protect mice against *S. aureus*. Leukocidin-based immunizations generate both leukocidin-neutralizing antibodies and Th1/Th17 responses, which collectively protect the host against *S. aureus* BSI. Altogether, this study demonstrates that leukocidins are crucial virulence factors employed by *S. aureus* to counter immune defenses and that targeting leukocidin-mediated immune evasion by vaccination leads to enhanced host-mediated protection.

Results

Leukocidins blunt the development of broadly neutralizing antibody responses against *S. aureus*

While all the leukocidins exhibit strong tropism toward human leukocytes, LukED and HlgAB are also active in murine models of *S. aureus* BSI (Alonzo et al., 2013; DuMont et al., 2013; Lubkin et al., 2019; Reyes-Robles et al., 2013; Spaan et al., 2013, 2015, 2014). Thus, we focused on the role of LukED and HlgAB in *S. aureus*–mediated immune subversion in vivo. Using a murine model of recurrent BSI in outbred Swiss Webster mice (Fig. 1 A), we investigated if and how these leukocidins affect the generation of host immunity in the context of active infection. Mice that were subjected to recurrent infection (Fig. 1 A) with *S. aureus* (WT) and an isogenic strain that lacks the leukocidins LukED and HlgAB (ΔΔ) exhibited similar levels of bacterial burden and had similar levels of total serum IgG (Fig. S1). Recurrently infected mice developed antibodies against various *S. aureus* secreted and surface proteins 7 d following the last infection (Fig. 1 B). As expected, WT-infected mice developed anti-leukocidin antibodies, and mice infected with the ΔΔ strain did not develop antibodies against LukE, LukD, HlgA, and HlgB (Fig. 1 C). Anti-leukocidin antibodies isolated from WT-infected mice were functional and protected primary human neutrophils (hPMNs) from leukocidin-mediated cytotoxicity (Fig. 1, D and E). The potency of the neutralizing anti-leukocidin antibodies in the serum of WT-infected mice increased between 21 d post-infection (dpi) and 35 dpi, representing the antibody response after primary infection and secondary infection, respectively (Fig. 1, D and E). These data demonstrate that mice can generate antibodies that neutralize the cytolytic activity of the leukocidins during recurrent infection.

To quantify the anti–*S. aureus* surface-associated antibodies developed after WT and ΔΔ infections, we performed binding assays with whole *S. aureus*. For these studies, *S. aureus* Δ*spa* Δ*sbi* was used, which lacks the major surface Ig-binding proteins; therefore, it does not bind antibodies nonspecifically (Pishchany et al., 2009; Romagnani et al., 1982; Zhang et al., 1998). Serially diluted sera from mock-infected, WT-infected, and ΔΔ-infected mice isolated at 35 dpi were incubated with *S. aureus* Δ*spa* Δ*sbi*, and the reactivity of the anti–*S. aureus* surface-associated antibodies was measured by flow cytometry. Serum from ΔΔ-infected mice had higher titers of anti–*S. aureus* antibodies than WT-infected mice (Fig. 1 F). These results suggest that leukocidins can reduce the titers of anti–*S. aureus* antibodies during BSI.

To evaluate if the antibody responses generated from recurrent BSI are protective, naive mice were passively immunized with pooled serum isolated 35 dpi from mice that were mock infected, WT infected, or ΔΔ infected. The passively immunized mice were then challenged i.v. with a lethal dose of *S. aureus* 24 h after serum transfer. Mice that received serum from mock-infected mice succumbed to infection in a leukocidin-dependent manner (Fig. 1 G; Alonzo et al., 2012; Lubkin et al., 2019). Surprisingly, mice that received serum from ΔΔ-infected mice did not exhibit protection (Fig. 1 G), even though the sera contained high levels of anti–*S. aureus* antibodies (Fig. 1 F). In contrast, mice that received serum from WT-infected mice exhibited increased survival when challenged with a lethal dose of WT *S. aureus* (Fig. 1 G). Although the sera from WT-infected mice contains fewer anti–*S. aureus* surface-associated antibodies (Fig. 1 F), these sera have leukocidin-neutralizing antibodies (Fig. 1, D and E) that are critical for protection in BSI. Altogether, these results suggest that leukocidins are an important component of the immune evasion strategy of *S. aureus*. They reduce the titer of anti–*S. aureus* antibodies generated by the host; however, they also enable the host to develop leukocidin-neutralizing antibodies, which can confer protection against subsequent BSI challenge in passively immunized mice.

Leukocidin-based immunizations protect against lethal methicillin-sensitive *S. aureus* (MSSA) and methicillin-resistant *S. aureus* (MRSA) BSIs

We hypothesized that inducing neutralizing antibodies against leukocidins through vaccination would interfere with the immune evasion strategy of *S. aureus* and protect the host from subsequent lethal infection. Thus, we implemented an active immunization protocol using recombinant leukocidin subunits. LukED and HlgAB share high protein sequence identity (Yoong and Torres, 2013). As with all bicomponent leukocidins, LukED and HlgAB require both the S-subunit (slow-eluting subunit) and the F-subunit (fast-eluting subunit) for cytotoxicity (Spaan et al., 2017). As such, immunization with WT leukocidins can be toxic to the host (Reyes-Robles et al., 2016; Lubkin et al., 2019). To overcome this potential limitation, we took advantage of the unique bicomponent nature of leukocidins and devised combinations of WT toxins with only the S-subunits (LukE/HlgA) or only the F-subunits (LukD/HlgB). Additionally, we previously developed "toxoid" versions of LukED and HlgAB, which have a small (3–4 amino acids) deletion in the stem domain of each subunit, rendering these toxoids unable to form pores on target cells (Reyes-Robles et al., 2016). Hence, immunization with the toxoids should generate neutralizing antibodies against the toxins without harming the host. We sought to compare and contrast the protective immunity elicited from three different immunization regimens: LukE/HlgA, LukD/HlgB, and toxoid mutants ($LukE^{mut}$, $LukD^{mut}$, $HlgA^{mut}$, and $HlgB^{mut}$). Each

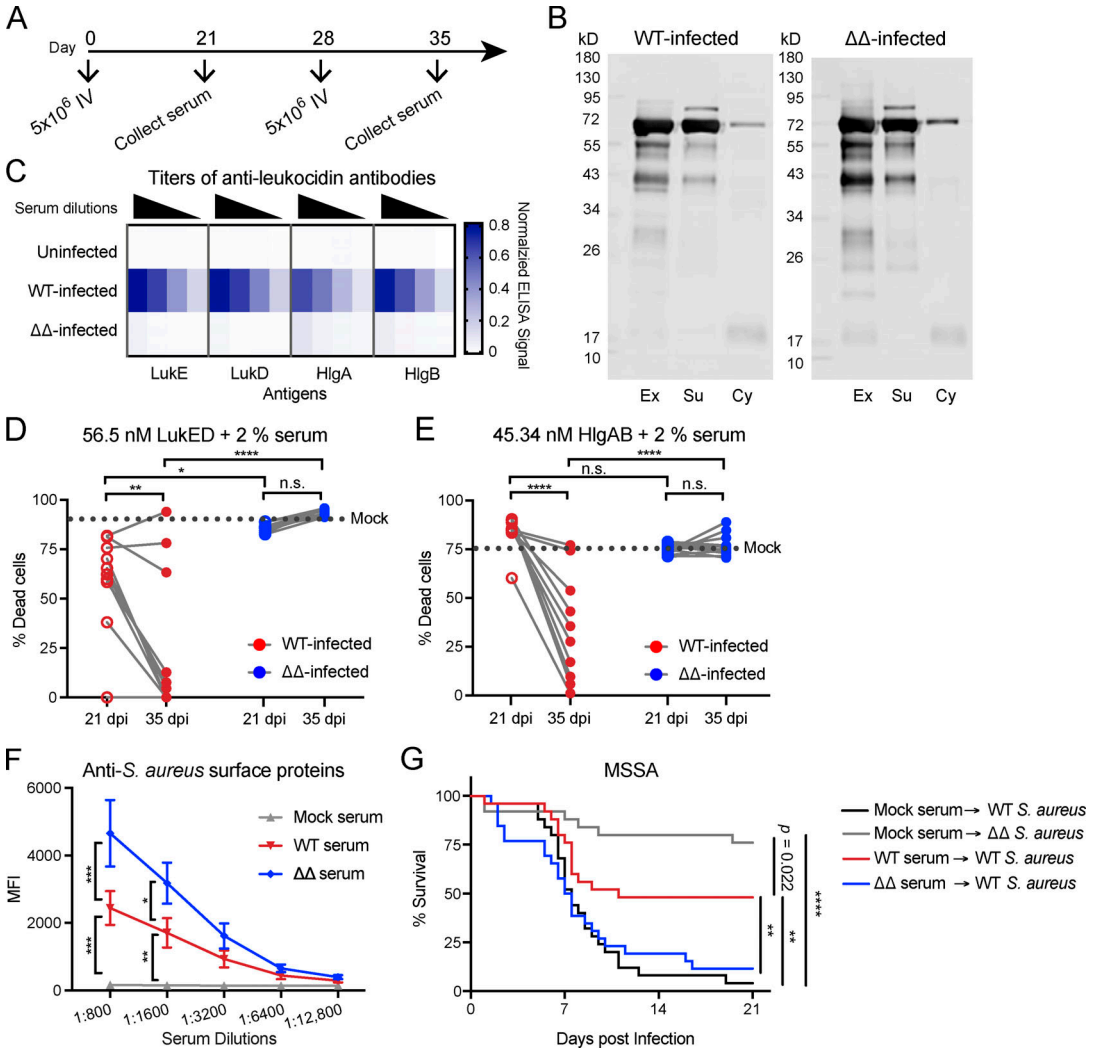

Figure 1. **Mice develop protective anti-leukocidin antibodies after recurrent infection. (A)** Schematic of the recurrent infection model. Mice were infected by retro-orbital infection with 5 × 10^6 CFU on days 0 and 28 with WT or isogenic Δ*lukED* Δ*hlgACB* (ΔΔ) *S. aureus* strain Newman, and sera were collected on day 21 and day 35 after infection. **(B)** Representative immunoblots of *S. aureus* exoproteins (Ex), surface proteins (Su), and cytoplasmic proteins (Cy) against pooled serum from mice infected with indicated *S. aureus* strains at 35 dpi. *n* = 3 independent experiments. **(C)** Heatmap representing the averaged normalized ELISA values of serial diluted serum isolated from uninfected mice and from mice infected with indicated *S. aureus* strains tested against purified LukE, LukD, HlgA, and HlgB. *n* = 9–13 mice per group. **(D and E)** Neutralization activity of serum antibodies using hPMNs intoxicated with LukED (D) or HlgAB (E). Dotted line indicates the averaged percent killing of hPMNs when toxins were preincubated with 2% heat-inactivated control serum (mock infected). Circles indicate the averaged percent killing of hPMNs when toxins were preincubated with 2% heat-inactivated serum from individual mice infected by the indicated strain. Cell viability was determined by the metabolic dye CellTiter. Statistical analysis was performed with two-way ANOVA, corrected with Sidak's multiple comparison. *n* = 9–13 mice per group and 4 hPMN donors. **(F)** Pooled serum described in G was incubated with Newman Δ*spa* Δ*sbi* to measure surface associated anti–*S. aureus* antibodies by flow cytometry. Graph depicts averaged median fluorescence intensity (MFI) ± SEM. Statistical analysis was performed with two-way ANOVA, corrected with Dunnett's multiple comparison. *n* = 4 independent experiments. **(G)** Naive mice were passive immunized with pooled serum isolated from mock-infected, WT-infected, or ΔΔ-infected mice 35 dpi. ~24 h after serum transfer, mice were infected by retro-orbital infection with 5 × 10^7 WT or ΔΔ *S. aureus* strain Newman. Morbidity of the animals was monitored for 21 d. Statistical analysis was performed with log-rank (Mantel-Cox) test corrected for multiple comparisons. *n* = 25 or 26 mice per group. *, P = 0.05; **, P < 0.01; ***, P < 0.001; ****, P < 0.0001. n.s., not significant.

protein mixture or buffer only (mock) was emulsified with the oil-in-water adjuvant "Titermax Gold" and administered subcutaneously to mice biweekly (Fig. 2 A). By day 49, mock-immunized mice did not have any evidence of antibodies against the leukocidins; however, LukE/HlgA–immunized mice developed a specific antibody response against LukE and HlgA; LukD/HlgB–immunized mice developed a specific antibody response against LukD and HlgB; and toxoid-immunized mice developed an antibody response against WT LukE, LukD, HlgA, and HlgB (Fig. 2 B). Notably, although the leukocidin subunits share similar protein structure and >30% protein sequence identity (Yoong and Torres, 2013), we did not observe cross-reactivity of the antibodies between the S- and F-subunits in the serum isolated from LukE/HlgA– and LukD/HlgB–immunized mice (Fig. 2 B).

Next, the titers and isotypes of the elicited anti-leukocidin antibodies were measured. Leukocidin-based immunization elicited high titers of IgG1, followed by that of IgG2b and IgG2a

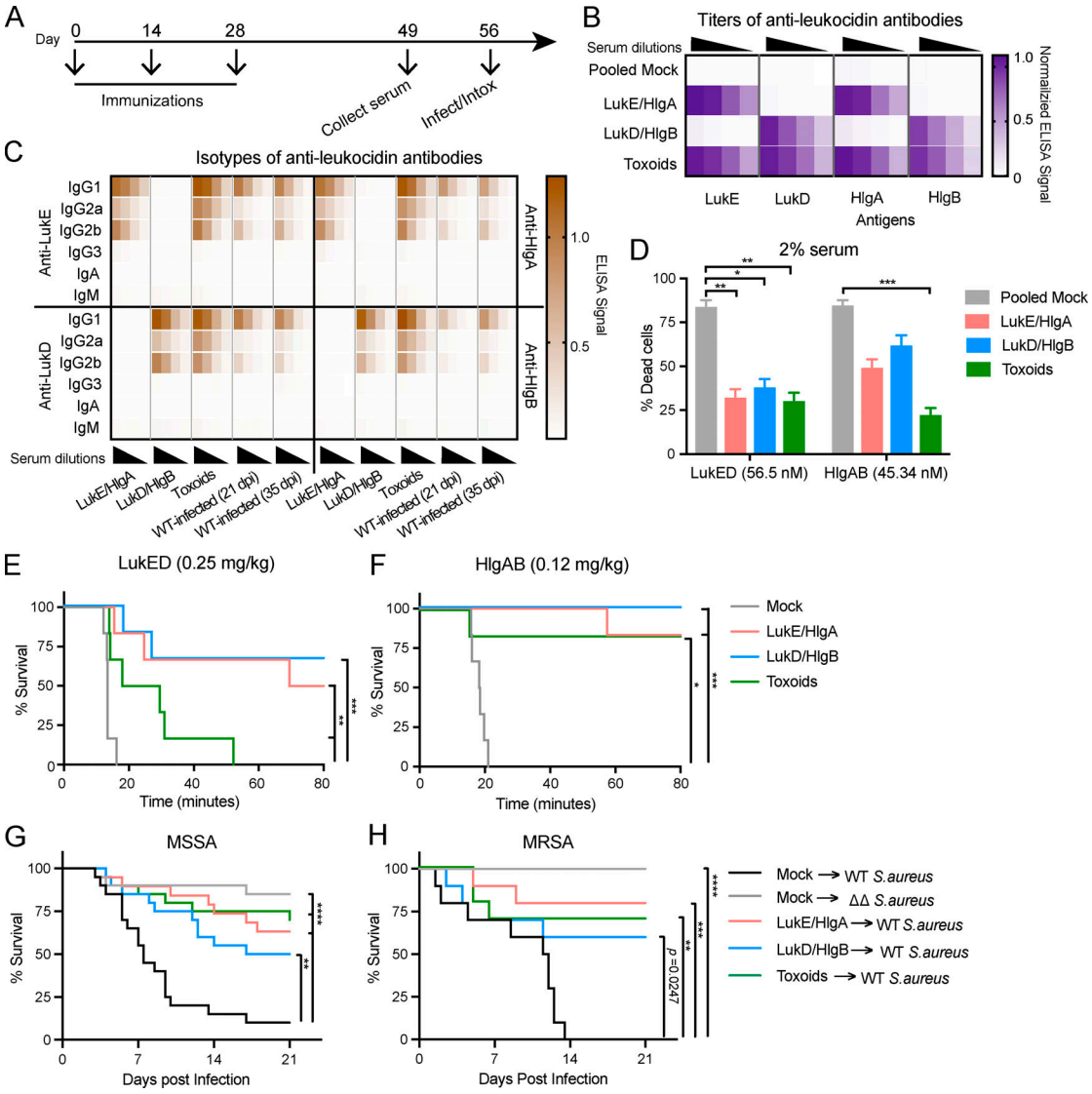

Figure 2. **Leukocidin-immunized mice develop protective immunity against *S. aureus*. (A)** Schematic for immunizations. Mice were immunized with the oil-in-water adjuvant Titermax Gold emulsified with buffer (mock) or with leukocidin cocktails of WT leukocidins: LukE/HlgA or LukD/HlgB and leukocidin toxoids: LukE^{mut}, LukD^{mut}, HlgA^{mut}, and HlgB^{mut} (toxoids). Sera were isolated on day 49. In vivo intoxication or infection studies were performed on day 56. **(B)** Heatmap representing averaged normalized ELISA values of serial diluted serum isolated from mock-immunized and the indicated leukocidin-immunized mice tested against purified LukE, LukD, HlgA, and HlgB. *n* = 25 or 26 mice per group. **(C)** Heatmap representing the averaged ELISA values of isotype-specific antibodies against LukE (top left), LukD (bottom left), HlgA (top right), and HlgB (bottom right) in serial diluted serum isolated from the indicated leukocidin-immunized mice on day 49 after immunization or WT-infected mice from Fig. 1 at 21 dpi representing humoral responses from primary infection and at 35 dpi representing humoral responses from secondary infection. *n* = 5 mice per group. **(D)** Neutralization activity of serum antibodies isolated from mock-immunized mice or the indicated leukocidin-immunized mice 49 d after immunization on hPMNs intoxicated with LukED or HlgAB. Cell viability was determined by the metabolic dye CellTiter. Bar graph depicts the averaged percent killing of hPMN + SEM. Statistical analysis was performed with two-way ANOVA, corrected with Dunnett's multiple comparison. *n* = 36–38 mice and 9 hPMN donors per group. **(E and F)** Mock-immunized or the indicated leukocidin-immunized mice were intoxicated with purified LukED (E) or HlgAB (F). Morbidity of the animals was monitored for 80 min. *n* = 6 mice per group. **(G and H)** Retro-orbital infection of mice was performed on mock-immunized or the indicated leukocidin-immunized mice with 5 × 10^7 MSSA Newman. *n* = 19 or 20 mice per group (G) or 2.5 × 10^7 MRSA USA500, 10 mice per group (H). Morbidity of the animals was monitored for 21 d. **(E–H)** Statistical analyses were performed with log-rank (Mantel-Cox) test corrected for multiple comparisons. *, P = 0.05; **, P < 0.01; ***, P < 0.001; ****, P < 0.0001.

antibodies (Fig. 2 C). While LukE/HlgA– and LukD/HlgB–immunized mice elicited more IgG2b anti-leukocidin antibodies than IgG2a, toxoid-immunized mice elicited similar titers of IgG2a and IgG2b antibodies. We did not detect IgG3, IgA, or IgM anti-leukocidin antibodies at the serum dilutions tested (Fig. 2 C). We also evaluated the antibodies generated from recurrent infection (Fig. 1) to compare the isotypes of anti-leukocidin antibodies elicited after infection and immunization. In contrast to immunization, the titers of anti-leukocidin antibodies generated from infections with the WT bacteria were lower (Fig. 2 C). However, similar to antibodies elicited from LukE/HlgA and LukD/HlgB immunization, infection with WT bacteria resulted in a high titer of anti-leukocidin IgG1, followed by IgG2b and IgG2a, and no detectable IgG3, IgA, and IgM (Fig. 2 C).

Next, we evaluated the ability of serum antibodies to neutralize the cytotoxic effects of LukED and HlgAB ex vivo using hPMNs. Serum from mock-immunized animals did not neutralize LukED or HlgAB, whereas serum from all three leukocidin-immunized groups protected hPMNs from the cytotoxic effect of the toxins (Fig. 2 D). In particular, serum from toxoid-immunized mice displayed highly potent neutralizing activity against LukED and HlgAB (Fig. 2 D).

The i.v. administration of purified LukED and HlgAB is lethal to mice (Lubkin et al., 2019; Reyes-Robles et al., 2016). Death is mediated by vascular leakage as a direct result of the toxins targeting the Duffy antigen receptor for chemokines on endothelial cells (Lubkin et al., 2019). We hypothesized that toxin-neutralizing antibodies in the serum would prevent toxins from targeting endothelial cells, thus reducing lethality during intoxication. To test this, we intoxicated mock- or leukocidin-immunized mice and monitored morbidity. Leukocidin-immunized animals exhibited increased survival when intoxicated with a lethal dose of LukED or HlgAB compared with the mock-immunized mice (Fig. 2, E and F), suggesting that vaccine-induced leukocidin-neutralizing antibodies protect mice in vivo. Indeed, when naive animals were passively immunized with pooled serum from mock- or leukocidin-immunized mice, only animals that received leukocidin-immunized serum were protected from intoxication (Fig. S2). Altogether, our data demonstrate that leukocidin-based immunization generates high titers of leukocidin-specific antibodies that potently neutralize the cytotoxicity of LukED and HlgAB in both ex vivo and in vivo models.

To evaluate if the immunity conferred by leukocidin-based immunizations is protective against lethal BSI, we infected mice i.v. with the MSSA strain Newman (Baba et al., 2008) or a MRSA USA500 strain (Benson et al., 2014). These two strains are highly cytotoxic to human neutrophils ex vivo and lethal to mice during BSI due to the high production of leukocidins (Alonzo et al., 2012; Benson et al., 2014; Chapman et al., 2017; DuMont et al., 2011; Lubkin et al., 2019). While mock-immunized animals succumbed to infection in a leukocidin-dependent manner, all three groups of leukocidin-immunized mice were significantly more protected than mock-immunized mice infected with WT bacteria (Fig. 2, G and H). Collectively, these results demonstrate that leukocidin-based immunization can protect mice from lethal *S. aureus* BSI.

Leukocidin-based immunizations promote bacterial clearance

To further dissect the breadth of protection elicited by the leukocidin-based immunization, we used a sublethal BSI model. Mock- and leukocidin-immunized mice were infected i.v. with *S. aureus*, and bacterial burden and gross pathology were examined at the acute phase of BSI (4 dpi) and the "chronic" phase of the infection (21 dpi). We observed lower bacterial burden in the kidneys and hearts of leukocidin-immunized mice than in mock-immunized mice infected with WT *S. aureus* at 4 and 21 dpi (Fig. 3, A–D). Strikingly, we observed a significant percentage of leukocidin-immunized mice that had no detectable bacterial burden in these organs (Fig. 3, E–H). The reduction in bacterial burden observed in leukocidin-immunized animals was also associated with decreased abscess formation in the kidneys compared with mock-immunized mice infected with either the WT or ΔΔ strain (Fig. 3 I). As an indicator of leukocidin-driven inflammation, mock-immunized mice infected with WT bacteria have larger kidneys and spleens than mice infected with the isogenic ΔΔ strain; leukocidin-immunized mice infected with WT bacteria are protected from leukocidin-driven inflammation in these organs as they have smaller kidneys and spleens, phenocopying mock-immunized mice infected with the isogenic ΔΔ strain (Fig. 3, J and K).

To expand the breadth of our findings, we next evaluated the protection of leukocidin-mediated immunization in a systemic peritonitis model of community-associated MRSA USA300 infection (Chan et al., 2019; Spaan et al., 2014). USA300 strains are responsible for the community-associated MRSA pandemic in the United States (Seybold et al., 2006). Toxoid-immunized mice exhibited reduced bacterial burden in the peritoneal lavage, liver, and lungs 3 dpi (Fig. 3 L). Altogether, these data demonstrate that leukocidin-based immunization protects mice from BSI by reducing bacterial burden, abscess formation, and inflammation (i.e., kidney and spleen size).

Immunization with leukocidins reduces the systemic inflammation observed upon *S. aureus* BSI

To evaluate the systemic inflammatory state of the immunized mice after BSI, serum was isolated from mice before infection, 4 dpi, and 21 dpi. The concentrations of 16 serum cytokines were measured (Fig. S3), the averaged concentration of the individual cytokine for each group was normalized, and the data were organized by unsupervised hierarchical clustering to demonstrate relatedness of serum cytokine profiles of each group at the different infection time points (Fig. 4). The unsupervised hierarchical clustering resulted in the separation of uninfected mice from mice that had been infected for 4 d: uninfected mock- and leukocidin-immunized mice had similar baseline levels of cytokines and were clustered together. During the acute phase of infection (i.e., 4 dpi), the innate immune system responded to the presence of *S. aureus* by inducing high levels of proinflammatory cytokines, such as KC, IL6, IFNγ, IP10, and MIG (Fig. 4). Of note, mock-immunized mice infected with WT bacteria had elevated levels of these inflammatory cytokines compared with mock-immunized mice infected with the ΔΔ strain, suggesting that the leukocidins may be important drivers of elevated cytokine levels during the acute phase of infection (Fig. 4).

In contrast to the acute infection, the cytokine profiles of mice 21 dpi did not cluster together. The profiles of mock-immunized mice infected with WT or ΔΔ *S. aureus* and LukD/HlgB–immunized mice infected with WT *S. aureus* were more similar to the acutely infected mice. In contrast, the cytokine profiles of LukE/HlgA– and toxoid-immunized mice returned to baseline levels similar to uninfected mice on 21 dpi and were clustered together with the uninfected mice (Fig. 4). These data demonstrate that immunization with the leukocidins can lead to a lower systemic inflammatory state upon *S. aureus* BSI.

Leukocidin-elicited antibody and T cell responses are required for host protection

We demonstrated in Fig. 1 G that serum from WT-infected mice conferred protection to naive mice during BSI. Therefore, we

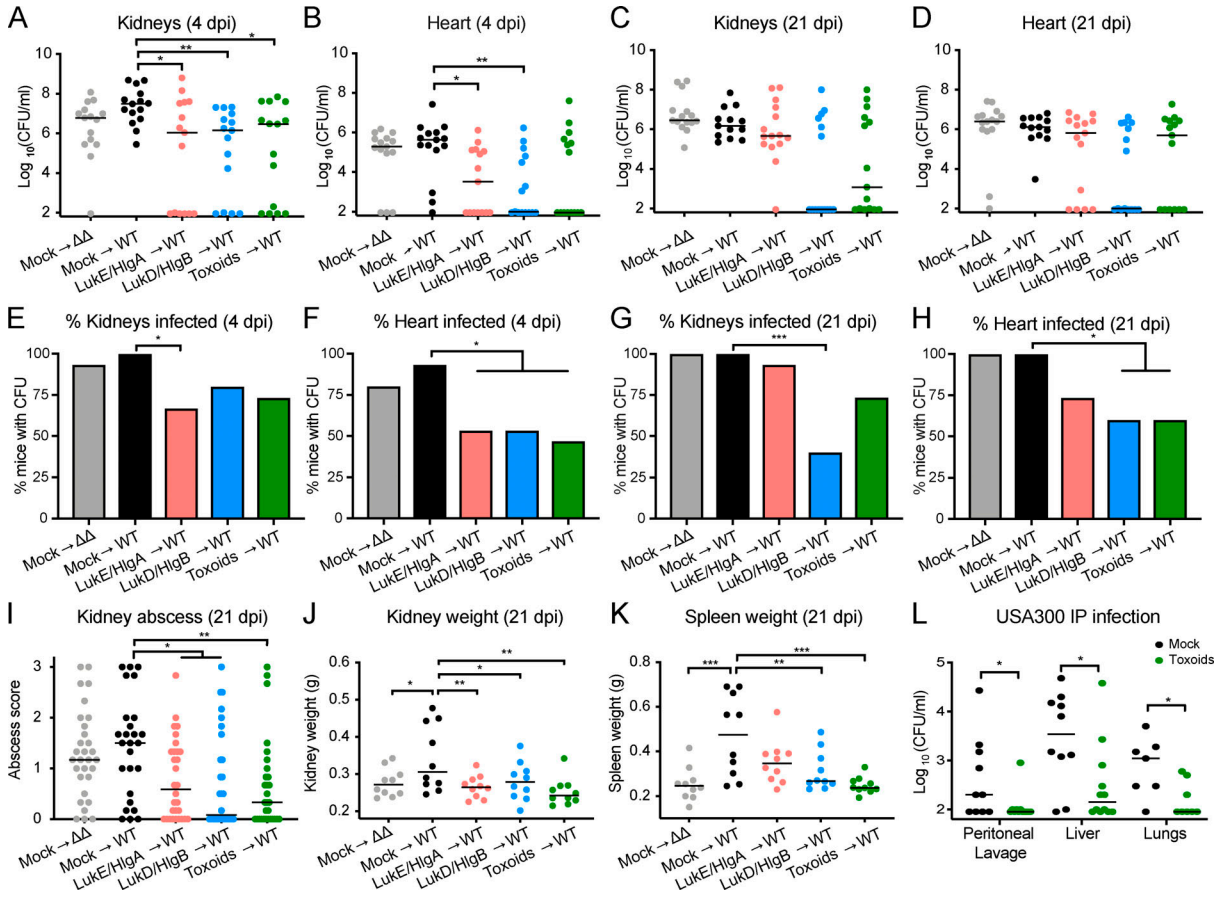

Figure 3. **Leukocidin-immunized mice have lower bacterial burden and organ pathology after *S. aureus* systemic infection.** Mock-immunized or leukocidin-immunized mice were infected IV with 5×10^6 WT or ΔΔ *S. aureus* strain Newman. **(A–D)** Bacterial burdens in kidneys and hearts were enumerated on 4 dpi (A and B) and 21 dpi (C and D). Each circle represents an individual mouse; lines depict the median bacterial burden of the indicated organ. Statistical analyses were performed with Kruskal-Wallis test, corrected with Dunnett's multiple comparison. *n* = 13–15 mice per group. **(E–H)** Bar graphs depict the percentages of mice from A–D with detectable bacterial burden in the indicated organ. Statistical analyses were performed with Fisher's exact tests. **(I)** Abscess severity of individual kidneys was scored by six independent blind observers. Each circle indicates the averaged disease score of a kidney. Lines indicate the median score per group. *n* = 26–30 kidneys from 13–15 mice per group. **(J and K)** Weights of kidneys (J) and spleens (K) from mock- or leukocidin-immunized mice at 21 dpi. Each circle represents an individual mouse; lines indicate the median weight of the indicated organ. *n* = 10 mice per group. Statistical analyses were performed with one-way ANOVA, corrected with Dunnett's multiple comparison. **(L)** Bacterial burden of mice infected with USA300 strain SF8300 i.p. at 8×10^7 CFU. Each circle represents an individual mouse; lines depict the median bacterial burden of the indicated organ. *n* = 7–12 mice per group. Statistical analyses were performed with the Mann-Whitney test. *, P = 0.05; **, P < 0.01; ***, P < 0.001.

investigated if sera isolated from leukocidin-immunized mice can protect naive animals against BSI. We performed passive immunization of naive mice with pooled serum isolated from mock- or leukocidin-immunized mice. After ~24 h, the mice were challenged with a lethal dose of *S. aureus*. Mice that received serum isolated from LukE/HlgA–, LukD/HlgB–, or toxoid-immunized mice did not exhibit significant protection compared with mice that received serum from mock-immunized mice (Fig. 5 A). These results suggest that anti-toxin antibodies alone are insufficient for protection from *S. aureus* BSI and that additional immune components elicited during vaccination are required for protection.

Besides toxin-neutralizing antibodies, we hypothesized that leukocidin-based immunization generates leukocidin-specific memory T cells that respond to the presence of leukocidins during infection. The effector functions of these toxin-specific T cells can promote phagocytic killings and activate other immune effector functions, ultimately contributing to bacterial clearance in organs (Ellis and Beaman, 2004; Ishigame et al., 2009; Lin et al., 2009; Monaci et al., 2015; Nakai et al., 2017; Nathan et al., 1983). To test this hypothesis, we depleted CD4 T cells during the course of vaccination (Fig. S4, A–C). We found that CD4 T cell depletion caused a reduction in the titers of anti-leukocidin antibodies, and the ability of the serum to neutralize leukocidin cytotoxicity was abolished (Fig. S4, D and E). Toxoid-immunized mice that were depleted of CD4 T cells had reduced protection from lethal *S. aureus* BSI compared with toxoid-immunized mice that were treated with the isotype control antibody (Fig. S4 F).

To evaluate the immunization-driven antigen-specific memory T cell response to leukocidins, we stimulated splenocytes from mock- or toxoid-immunized mice with LukE, LukD, HlgA, or HlgB and measured the concentration of secreted cytokines. While splenocytes from mock- and toxoid-immunized

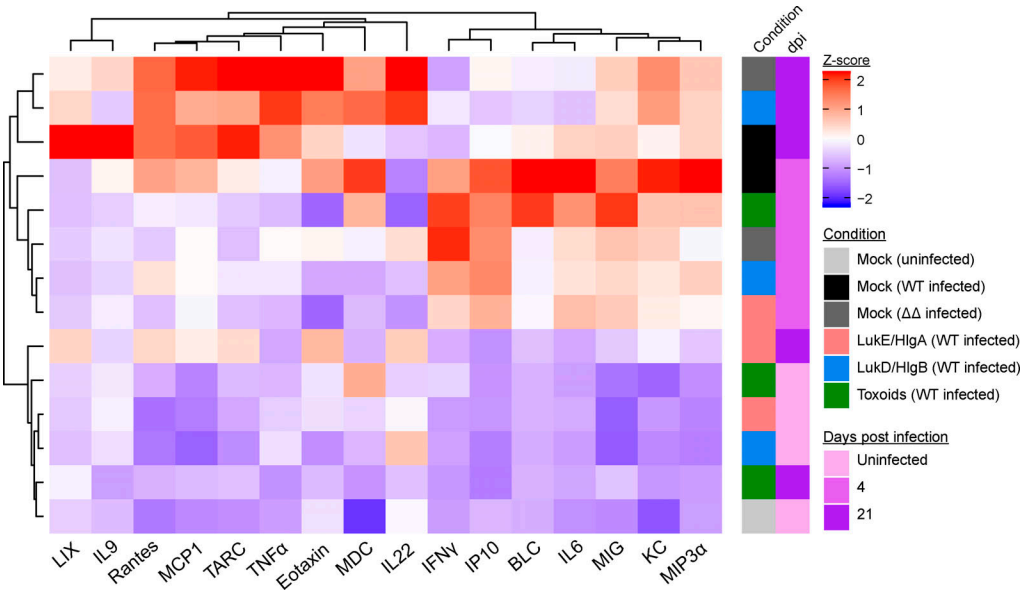

Figure 4. **Leukocidin-immunized mice are in a lowered inflammatory state after *S. aureus* systemic infection.** Heatmap depicts the unsupervised hierarchical clustering of z-score normalized averaged serum concentrations of the indicated cytokines from mock-immunized or the indicated leukocidin-immunized mice at 7 d before infection (uninfected), 4 dpi, and 21 dpi. *n* = 20 mice per group for uninfected mice, 15 per group for 4 dpi, and 4 or 5 mice per group for 21 dpi.

mice produced similar levels of cytokines when cultured with media, we found that splenocytes from toxoid-immunized mice produced significantly higher levels of TNFα, IFNγ, IL2, IL4, IL5, IL10, IL6, IL17a, IL17f, and IL22 compared with the splenocytes from mock-immunized mice when cultured with the antigen (Fig. 5, B and C; and Fig. S5). Splenocytes from toxoid-immunized mice exhibit a >100-fold increase in the production of IFNγ and IL17a upon leukocidin stimulation over media control (Fig. 5, B and C; and Fig. S5, A and B). Furthermore, we identified CD4 and CD8 T helper cells from toxoid-immunized mice as producers of IFNγ upon antigen stimulation, while cells from mock-immunized mice exhibited negligible induction (Fig. 5, D and E). We also observed that toxoid-immunized mice harbor more IL17-producing CD4 and CD8 T cells than mock-immunized mice regardless of culture conditions (Fig. 5, F and G). These results demonstrate that immunization with leukocidins elicits toxin-specific T cells that produce cytokines involved in Th1- and Th17-mediated immunity.

IFNγ and IL17 are important cytokines for anti–*S. aureus* immunity (Brown et al., 2015; Cho et al., 2010; Ishigame et al., 2009; Lacey et al., 2017; Lin et al., 2009; Narita et al., 2010; Zhao et al., 1998). IFNγ is an important cytokine for promoting phagocyte recruitment and activating phagocytes to enhance their bactericidal activities, including phagocytosis, oxidative burst, and nitric oxide production (Ellis and Beaman, 2004; Nathan et al., 1983). IL17, the principle cytokine produced by Th17 cells, is also an important cytokine involved in recruiting and activating neutrophils and macrophages (Ishigame et al., 2009; Miller and Cho, 2011; Nakai et al., 2017). Thus, we examined the effect of these cytokines in phagocyte-mediated *S. aureus* killing. We exposed primary bone marrow–derived macrophages (BMDMs) to culture supernatants from splenocytes of mock- or toxoid-immunized mice treated with media only or stimulated with toxoids. The primed BMDMs were then infected with *S. aureus* to measure phagocytic killing. While culture supernatants of toxoid-stimulated splenocytes from mock-immunized mice did not enhance BMDM-mediated killing of *S. aureus* compared with cells treated with media only, the culture supernatants of toxoid-stimulated splenocytes from toxoid-immunized mice boosted BMDM-mediated killing of *S. aureus* (Fig. 5 H). To directly assess the impact of IFNγ and IL17 on BMDM-mediated killing of *S. aureus*, BMDMs were preexposed to purified IFNγ and/or IL17 followed by infection with *S. aureus*. We found that although IFNγ or IL17 alone was not sufficient to boost BMDM phagocytic killing, the combination of both cytokines resulted in higher phagocytic killing of *S. aureus* (Fig. 5 I). Altogether, these data support the model that the IFNγ and IL17 produced by the leukocidin-specific T cells in response to leukocidin immunization enhance phagocytic killing of *S. aureus*. Hence, both cellular and antibody responses directed against leukocidins by vaccination contribute toward protection against subsequent *S. aureus* challenge.

Discussion

S. aureus leukocidins are widely recognized as professional leukocyte killers and are important virulence factors during *S. aureus* pathogenesis (Spaan et al., 2017). However, studies evaluating the effect of these toxins on the ability of the host to mount an adaptive immune response against the pathogen are lacking. Our data demonstrate that these toxins negatively impact the host antibody response toward *S. aureus* during infection. Moreover, we established that exploiting these toxins as vaccine antigens protects mice from *S. aureus* BSI. In our model, leukocidin-based immunization results in the production of

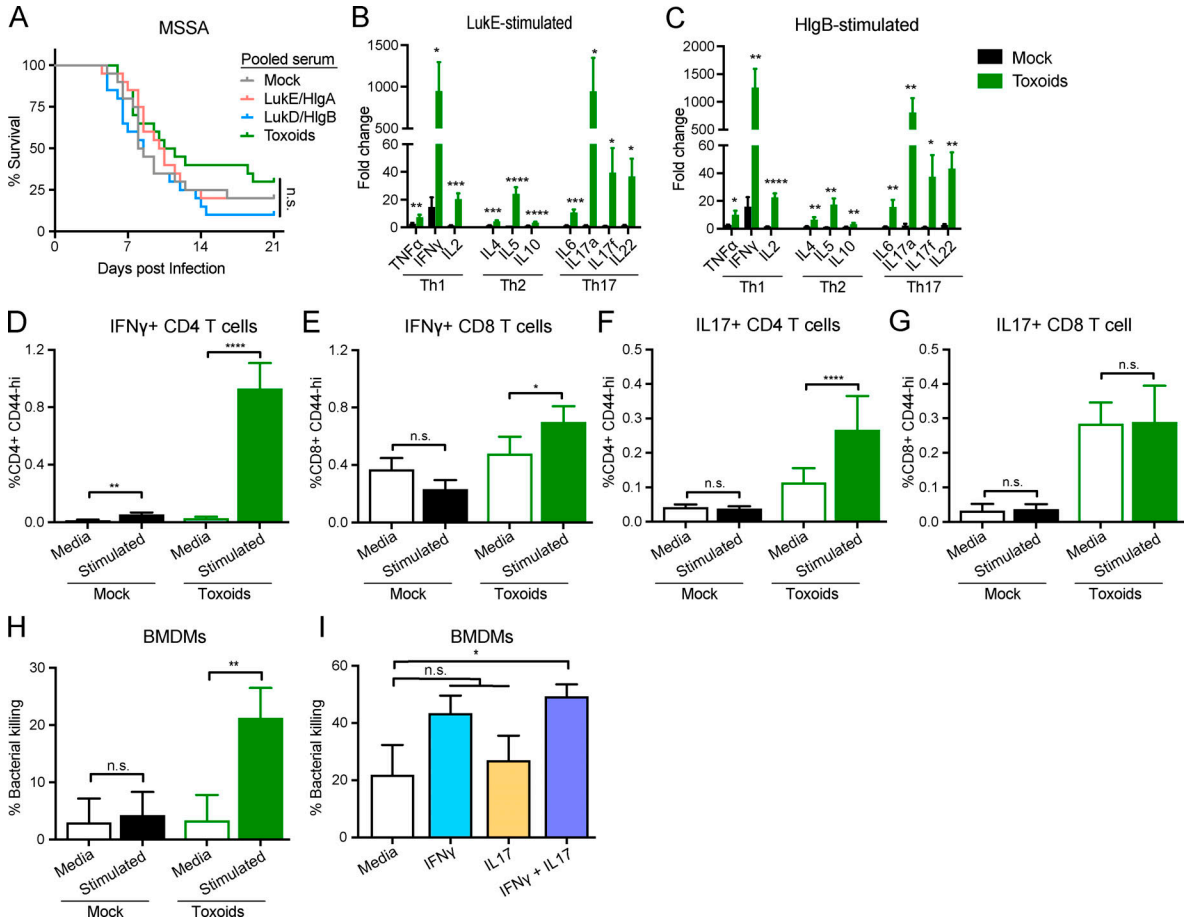

Figure 5. **Leukocidin-immunized mice require both humoral immunity and cell-mediated immunity for protection against *S. aureus* infections.** **(A)** Naive mice were passive immunized with pooled serum isolated from mock-immunized or the indicated leukocidin-immunized mice. ~24 h after serum transfer, mice were infected by retro-orbital infection with 5×10^7 WT *S. aureus* strain Newman. Morbidity of the animals was monitored for 21 d. Statistical analysis was performed with log-rank (Mantel-Cox) test corrected for multiple comparisons. n = 20 mice per group. **(B and C)** Splenocytes from mock- or toxoid-immunized mice were cultured with media and LukE (B) or HlgB (C). Culture supernatants were collected to measure the concentrations of secreted cytokines. Bar graphs depict averaged fold change of the indicated toxin-stimulated splenocytes over media-treated controls for the indicated cytokine + SEM. n = 10 mice per group. Statistical analyses were performed with unpaired Student's t test between the splenocytes from mock- and toxoid-immunized mice for each cytokine. **(D–G)** Flow cytometry analyses of IFNγ-producing CD44$^+$ CD4 T cells (D) and CD8 T cells (E) and IL17-producing CD44$^+$ CD4 T cells (F), and CD8 T cells (G) + SEM from the splenocytes from mock- or toxoid-immunized mice. Statistical analyses were performed with Wilcoxon tests. n = 20 mice per group. **(H)** BMDMs were primed with 10% culture supernatants from mock- or toxoid-immunized splenocytes for 4 h and then infected with *S. aureus* (Newman ΔΔΔΔ) at a multiplicity of infection (MOI) of 1 for 1 h. Bacterial CFUs were measured and compared against the input. Bar graph depicts the averaged percent killing of bacteria + SEM. Statistical analysis was performed with paired Student's t test. n = 10 splenocyte culture supernatants per group, each tested with BMDM from six mice per group in three independent experiments. **(I)** BMDMs were primed with recombinant IFNγ and/or recombinant IL17 for 4 h and then infected with *S. aureus* (Newman ΔΔΔΔ) at MOI of 1 for 1 h. Bacterial CFUs were measured and compared against the input. Bar graph depicts the averaged percent killing of bacteria + SEM. n = 8 mice per group, four independent experiments. Statistical analysis was performed with one-way ANOVA, corrected with Dunnett's multiple comparison. *, P = 0.05; **, P < 0.01; ***, P < 0.001; ****, P < 0.0001. n.s., not significant.

toxin-neutralizing antibodies and the generation of Th1/Th17 responses. Altogether, our data suggest that toxin-neutralizing antibodies prevent toxinosis, resulting in the enhanced survival of mice, while Th1/Th17 responses generate a cytokine environment rich in IFNγ and IL17 that increases phagocytic killing, resulting in the reduction of bacterial burden. Collectively, our study demonstrates the importance of targeting immune subversion factors in an anti–*S. aureus* vaccine and highlights the synergistic effect of antigen-specific T cell responses and neutralizing antibodies in promoting host protection against *S. aureus* BSI.

Anti–*S. aureus* antibodies are detected in the sera of patients infected with *S. aureus*. Among patients with *S. aureus* infections, many of these highly reactive antibodies are directed against antigens that contain a signal peptide, indicating that these proteins are targeted toward the cell surface or are secreted (Radke et al., 2018). Antibodies targeting the leukocidins, which are secreted virulence factors, are detected in the serum of patients (Adhikari et al., 2012; Thomsen et al., 2014; Pelzek et al., 2018; Radke et al., 2018). In particular, toxin-neutralizing antibodies against the leukocidins LukAB and Panton-Valentine leukocidin were recovered from sera isolated from children with *S. aureus* infections (Hermos et al., 2010; Thomsen et al., 2014). We demonstrate that similar to humans, mice subjected to recurrent invasive infections

(i.e., BSIs) developed anti–*S. aureus* antibodies that can neutralize LukED and HlgAB.

During infections, neutrophils, monocytes, macrophages, dendritic cells, and memory T cells are thought to be targeted by the leukocidins (Spaan et al., 2017). A close relative of the bicomponent leukocidins, α-toxin, also exhibits leukocidal activity and was recently shown to suppress antigen-specific T cell responses (Lee et al., 2020). Although these toxins suppress host adaptive immunity against *S. aureus,* exposure to these virulence factors during the initial infection is crucial for the development of neutralizing antibodies (Zhao et al., 2015). In our study, toxin-neutralizing antibodies generated through recurrent BSIs are necessary to protect naive mice from lethal *S. aureus* BSI challenges (Fig. 1 G). As such, the expression of toxins and other immune subversion factors is important in directing the host adaptive immune responses.

Our study highlights the importance of targeting immune modulatory factors as vaccine antigens. Leukocidin-based immunization prevents the cytotoxic and immune suppressive effects of the toxins in vivo and provides the host with protection during BSI. However, the protective effect of a leukocidin-based vaccine is limited to *S. aureus* strains that can produce leukocidins; therefore, additional antigens must be explored to extend protective efficacy to strains that produce little to no toxins (i.e., *agr* mutants; Alonzo et al., 2012; Dunman et al., 2001). Besides the bicomponent leukocidins, other immune subversive factors such as staphylococcal protein A (SpA) and α-toxin were explored previously as potential vaccine antigens. The production of SpA reduces host antibody repertoire (Goodyear and Silverman, 2003; Keener et al., 2017; Pauli et al., 2014), while α-toxin targets ADAM-10–expressing cells for lysis via a pore-formation mechanism similar to the bicomponent leukocidins (Spaan et al., 2017; Wilke and Bubeck Wardenburg, 2010). Vaccination against these immune subversive factors (i.e., the leukocidins, SpA, and α-toxin) boosts the host's ability to defend against *S. aureus* infections (Kennedy et al., 2010; Kim et al., 2010). The findings from our study and others on the protective effect of vaccinating against immune subversion factors have important implications for formulating an efficacious anti–*S. aureus* vaccine: immunity against such immune modulatory factors not only inhibits the biological activity of the virulence factor (i.e., via antibody neutralization), but the effect of this virulence factors on the host can also be reversed or inhibited.

The lack of BSI protection conferred by immune sera containing potent toxin-neutralizing antibodies (Fig. 5 A) corroborates the recent failure of ASN-100, a pan–pore-forming toxin (i.e., bicomponent leukocidins and α-toxin) neutralizing antibody formulation, after a Phase II clinical study (ClinicalTrials.gov, 2019). This also highlights an underappreciated role of memory T cell responses toward host protection. In our leukocidin-based vaccination model, host protection was mediated by the synergistic relationship of antigen-specific T cell responses and the production of neutralizing antigen-specific antibodies. Our study further corroborates the finding that CD4 depletion during vaccination abolishes the protective effect of immunization against *S. aureus* invasive infections (Monaci et al., 2015). High-affinity neutralizing antibodies require the help of CD4 T cells. As such, CD4 depletion during vaccination also impairs the quality of antigen-specific antibody production. Future studies should delineate how the different subtypes of CD4 T cells, CD8 T cells, and B cells participate toward host protection during *S. aureus* infection. These findings will have important implications for vaccine design: the identification of the specific T cell immune responses required for host protection will help guide the design and selection of a vaccine adjuvant that will elicit the ideal immune response for maximal protection.

In our study, we identified the leukocidins as potent inducers of Th1/Th17 immune responses. Th1/Th17 immunity is crucial for bacterial clearance and promotes host protection against *S. aureus* infections (Brown et al., 2015; Cho et al., 2010; Ishigame et al., 2009; Lacey et al., 2017; Lin et al., 2009; Narita et al., 2010; Zhao et al., 1998). Moreover, the effector cytokines IFNγ for Th1 immunity and IL17 for Th17 immunity have been shown to be important for vaccine-mediated protection against *S. aureus* in murine models (Lin et al., 2009). We showed that the cytokine environment engendered by Th1/Th17 memory cells enhance phagocytic killing of *S. aureus*. Based on our results and the known "helper" properties of IFNγ and IL17 (Ellis and Beaman, 2004; Ishigame et al., 2009; Nakai et al., 2017; Nathan et al., 1983), we postulate that in the leukocidin-immunized mice, these effector cytokines promote the recruitment and activation of phagocytes for bacterial clearance, while toxin-neutralizing antibodies act to prevent leukocidin-mediated killing of these immune cells (Fig. 6).

The failures of past anti–*S. aureus* vaccine trials highlight the complexity of *S. aureus* pathogenesis and emphasize the importance of much-needed research into *S. aureus*–host interactions. Equally important is the fact that many potent *S. aureus* immune evasion factors (e.g., superantigens, CHIPS, LukSF-PV, and LukAB) exhibit strong tropism toward humans and have limited activities in commonly used preclinical animal models (Salgado-Pabón and Schlievert, 2014; Spaan et al., 2017). We posit that a successful anti–*S. aureus* vaccine should include antigens that elicit antibody and T cell responses that will restrain the bacterium's ability to evade host immune defenses while promoting clearance of the bacterium. This study identifies the leukocidins as potential vaccine antigens that lead to disarmament of the bacteria and activation of antibody and T cell responses, ultimately resulting in enhanced host protection.

Materials and methods

Ethics statement

All animal experiments were reviewed and approved by the Institutional Animal Care and Use Committee of New York University Langone Health. All experiments were performed according to National Institutes of Health guidelines, the Animal Welfare Act, and US federal law.

Leukopaks were obtained from de-identified healthy adult donors with informed consent from the New York Blood Center. De-identified samples are exempted from ethics approval requirements by the New York University Langone Health Institutional Review Board.

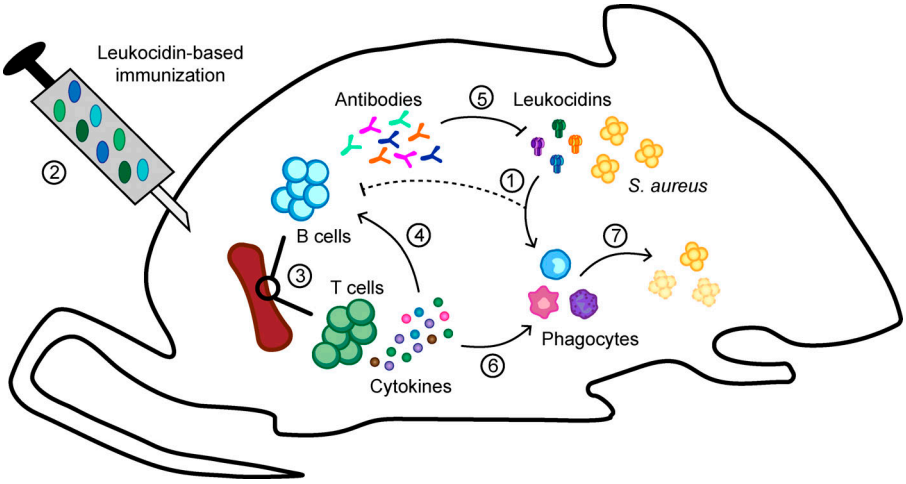

Figure 6. **Model of leukocidin-based immune evasion and protection by vaccination.** *S. aureus* produces leukocidins during infection that kill immune cells necessary for host defense and proper development of immunity (1). By immunizing mice with leukocidins (2), toxin-specific memory T cells and B cells (3) are developed. Helper T cells in the spleen (4) facilitate the maturation of B cells to produce toxin-neutralizing antibodies (5) that prevent leukocidin-mediated cytotoxicity. Additionally, Th1 and Th17 immunity developed as the result of leukocidin-based immunization produces IFNγ and IL17 (6) when the host reencounters the leukocidins during infections (7), which helps to simulate phagocytes to become better killers of *S. aureus*.

Bacterial strains and growth conditions

S. aureus strains are described in Table S1 and were grown on tryptic soy agar (Thermo Fisher Scientific) plates at 30°C–37°C and used within 1–2 wk on plate. Single colonies were inoculated to 5 ml tryptic soy broth (TSB; Thermo Fisher Scientific) in 15-ml conical tubes and grown at 37°C with 180-rpm shaking overnight and then subcultured at 1:100 in fresh media as indicated below.

Leukocidin purification from *S. aureus*

WT leukocidins and leukocidin toxoids were generated and purified as described previously (Reyes-Robles et al., 2016). When required, leukocidins were concentrated using concentrator columns (Ultra-15 Centrifugal Filter Units 10,000 nominal molecular weight limit, 15-ml volume capacity; EMD Millipore Amicon) before measuring protein concentration using absorbance at 280 nm with a Nanodrop (Thermo Fisher Scientific) and Beer-Lambert's equation. 2 µg of the purified proteins was separated by SDS-PAGE at 90 V for 120 min, followed by Coomassie Blue staining to visualize the proteins and to confirm purity.

Recurrent BSI model

5-wk-old female Swiss Webster mice (Hsd:ND4; Envigo) were anesthetized with ketamine/xylazine by i.p. injection and infected with *S. aureus* Newman (#2.97; VJT) and Newman Δ*lukED* Δ*hlgACB*::*tet* (#21.92; VJT) on day 0 and day 28 with 5×10^6 CFU by retro-orbital injection. On day 21, mice were bled by submandibular bleeding to collect serum. On day 35, mice were terminally bled by submandibular bleeding or cardiac puncture. Blood was collected in serum collector tubes (BD Biosciences), allowed to coagulate at room temperature (RT) for at least 30 min, and then centrifuged for 2 min at 15,000 rpm. Sera were stored at −80°C until use.

Total serum IgG measurement

Total serum IgG concentration was measured using the Mouse IgG Total Ready-SET-Go ELISA kit (eBioscience). Briefly, ELISA plates (Corning) were coated with 100 µl/well of capture antibody in 1× PBS overnight at 4°C and washed two times with wash buffer (1× PBS with 0.05% Tween-20). The plates were blot dried and blocked with blocking buffer (1× PBS with 0.05% Tween-20 and 0.5% BSA) for 2 h. The plates were washed two times with wash buffer. 100 µl of IgG standards and diluted serum samples were added to the plates. 50 µl of detection antibodies was added to all wells and incubated at RT for 3 h, followed by three washes with wash buffer. 100 µl of tetramethylbenzidine was added to each well and incubated for 15 min at RT, and then 100 µl of stop solution (2N H_2SO_4) was added to each well. The plates were read at 450 nm. Final serum concentrations were calculated by interpolating sample values using the standard curve and multiplying by the dilution factor.

Preparation of *S. aureus* protein fractions

S. aureus lysates were obtained from 5-h 1:100 subcultures of Newman Δ*spa* Δ*sbi* (#4.69; VJT) grown in TSB. Cells were pelleted by centrifugation at 4,000 rpm for 10 min. Culture supernatants were filtered by 0.22-µm syringe filter to remove cell debris. To obtain the exoprotein fractions, 1 ml of culture supernatant was precipitated using 110 µl of TCA overnight at 4°C. To obtain the noncovalent cell wall–associated proteins, cell pellets were washed once with 1× PBS and resuspended in 2.5 ml of noncovalent cell wall protein buffer (1.5 M LiCl and 25 mM Tris-HCl, pH 8.0) for 30 min on ice. The cells were centrifuged at 4,000 rpm for 10 min at 4°C. Supernatants containing noncovalent cell wall–associated proteins were collected and kept on ice. The cell pellet was then resuspended in 2.5 ml of covalent cell wall protein buffer (0.8 µg/ml lysostaphin in Tris-sucrose-$MgCl_2$ buffer (TSM; 50 mM Tris, 0.5 M sucrose, and 10 mM $MgCl_2$, pH 8.0) at RT for 10 min with nutating. The cells were centrifuged at 4,000 rpm for 10 min at 4°C. Supernatants containing cell wall proteins were collected and combined with the noncovalent cell wall protein fraction and filtered by 0.22-µm syringe filter to remove cell debris to obtain the surface protein fraction. To obtain the surface protein lysates, 1 ml of the surface protein fraction was precipitated using 110 µl of TCA overnight at 4°C. To obtain the cytoplasmic protein fraction, cell pellets were washed once with TSM buffer. The cell pellets were lysed with 5 ml of the cytoplasmic protein buffer (50 mM Tris-HCL and 20 mM $MgCl_2$, pH 7.5, containing DNase I and RNase I) for 20 min at RT. The cells were centrifuged at 4,000 rpm for

10 min at 4°C. Supernatants containing cytoplasmic proteins were collected and filtered by 0.22-µm syringe filter to remove cell debris. To obtain cytoplasmic protein lysates, 1 ml of the cytoplasmic protein fraction was precipitated using 110 µl of TCA overnight at 4°C. All TCA-precipitated samples were washed with 100% ethanol and dried at RT the following day. Protein pellets were resuspended in 20 µl of 8-M urea for 30 min at RT to dissolve the pellet, and 20 µl of 2× SDS buffer was added to the samples and boiled for 10 min. The samples were cooled to RT and stored at −80°C until use.

Immunoblotting against *S. aureus* proteins

For immunoblotting with *S. aureus* protein fractions, 5 µl of lysates from each *S. aureus* protein fraction was loaded onto 12% SDS-PAGE gels. For immunoblotting with purified leukocidin subunits, 5 µl of 500 ng of the indicated leukocidin subunits was loaded onto 12% SDS-PAGE gels. The proteins were separated by SDS-PAGE at 90 V for 120 min and then transferred onto nitrocellulose membranes at 1 A for 1 h. The membranes were blocked with 5% milk in PBST (1× PBS with 0.1% Tween-20 and 0.01% sodium azide) for 1 h at RT with nutating. Membranes were probed with the indicated serum at 1:1,000 dilution in PBST with 5% milk for overnight at 4°C. Membranes were washed three times with PBST with 10-min incubation during each wash and probed with Alexa Fluor 680 goat anti-mouse IgG (Life Technologies) at 1:25,000 dilution in PBST with 5% milk and 1% SDS for 1 h. Membranes were washed three times with PBST for 10 min and imaged using the Odyssey infrared imaging system (Li-Cor Biosciences).

Anti-leukocidin antibody titer measurement

Immunlon 2HB flat-bottom microtiter plates (Thermo Fisher Scientific) were coated with 1 µg/ml of the indicated antigen. The antigen-coated plates were blocked using 2% milk in PBS containing 0.05% Tween-20 for 1 h at RT. 50 µl of serial diluted serum (1:200; 1:800; 1:3,200; 1:12,800) was added to the ELISA plates and incubated at RT for 1 h with rocking, followed by three washes of 100 µl/well PBST. Then, 50 µl of HRP-conjugated goat anti-mouse IgG (H+L; 1:1,000; Bio-Rad Antibodies) or HRP-conjugated isotype-specific antibodies: goat anti-mouse IgG1 (1:8,000; Bio-Rad Antibodies), goat anti-mouse IgG2a (1:4,000; Bio-Rad Antibodies), goat anti-mouse IgG2b (1:8,000; Bio-Rad Antibodies), goat anti-mouse IgG3 (1:3,000; Bio-Rad Antibodies), goat anti-mouse IgA (1:3,000; Bio-Rad Antibodies), or goat anti-mouse IgM (1:3,000; Bio-Rad Antibodies) was added to each well and incubated at RT for 1 h with rocking, followed by three washes of 100 µl/well PBST. 50 µl of tetramethylbenzidine solution (Thermo Fisher Scientific) was added to each well and developed for 3 min exactly, followed by the addition of 50 µl of 2N H_2SO_4. The plates were read at absorbance of 450 nm using an EnVision 2103 Multilabel Reader (PerkinElmer).

Leukocidin-neutralization assays

Mouse sera were heat-inactivated at 55°C for 1 h. The heat-inactivated sera were serially diluted in 1× PBS and premixed with LukED or HlgAB for 30–60 min at RT. hPMNs were isolated from Leukopaks from the New York Blood Center using Dextran gradient followed by a Ficoll-Paque PLUS gradient (GE Amersham) as described previously (Reyes-Robles et al., 2016). hPMNs were plated at 200,000 cells/well in RPMI medium 1640 (Cellgro) supplemented with 10% heat-inactivated FBS and then intoxicated with the serum/leukocidin mixture for 1 h at 37°C with 5% CO_2. Cell viability was measured using the CellTiter 96 AQueous ONE Solution Cell Proliferation Assay (Promega). CellTiter was added to cells at a final concentration of 10% per well and incubated for 2 h at 37°C with 5% CO_2. Absorbance at 492 nm was measured using the EnVision 2103 Multilabel Reader.

Measuring anti–*S. aureus* surface antibody titers

Newman Δ*spa* Δ*sbi* was subcultured at 1:100 from an overnight culture in TSB for 3 h at 37°C with shaking. Bacteria were centrifuged at 4,000 rpm for 10 min and washed two times with 1× PBS. Bacteria were OD normalized to ~10^9 CFU/ml. To detect total anti–*S. aureus* surface protein antibodies on whole bacteria, the bacteria were diluted in FACS buffer (2% FBS and 0.05% sodium azide in 1× PBS) to ~1×10^7 CFU/ml and stained with a serial dilution of the indicated pooled serum for 30 min on ice. Bacteria were washed twice with FACS buffer and stained with PE goat anti-mouse IgG (1:200; Biolegend) for 30 min on ice. Bacteria were washed twice with FACS buffer and then fixed with FACS fixing buffer (2% paraformaldehyde in FACS buffer). Samples were acquired on the Cytoflex instrument (Beckman Coulter).

Leukocidin-based active immunization

4-wk-old female Swiss Webster mice or 5-wk-old female C57BL/6 mice were anesthetized with ketamine/xylazine by i.p. injection. 100 µl of 10 µg of LukE and 10 µg of HlgA (LukE/HlgA), or 10 µg of LukD and 10 µg of HlgB (LukD/HlgB), or 10 µg each of $LukE^{mut}$, $LukD^{mut}$, $HlgA^{mut}$, and $HlgB^{mut}$ (toxoids) in 1× Tris buffered saline with 10% glycerol was emulsified in Titermax Gold by vortexing for 5–10 min and then injected subcutaneously to the left flank on day 0. For subsequent booster immunizations, alternating flanks were injected subcutaneously on days 14 and 28. Mice were bled by submandibular bleeding on day 49. Blood was collected in serum collector tubes (BD Biosciences), allowed to coagulate at RT for at least 30 min, and then centrifuged for 2 min at 15,000 rpm. Sera were stored at −80°C until use.

Passive immunizations

Naive 5-wk-old female Swiss Webster mice received 200 µl of the indicated pooled serum by i.p. injection. ~24 h later, infection or intoxications were performed on the mice as described below.

In vivo intoxications

Mice were anesthetized with isoflurane by inhalation and then challenged with either 0.25 mg/kg of LukED or 0.12 mg/kg of HlgAB by retro-orbital injection. Signs of morbidity were monitored for 80 min after intoxication as done previously (Lubkin et al., 2019; Reyes-Robles et al., 2016).

In vivo infections

The indicated *S. aureus* strains were subcultured in TSB at 1:100 for 3 h at 37°C with shaking. Bacteria were centrifuged at

4,000 rpm for 10 min and washed two times with 1× PBS. The bacteria were OD normalized to ~10^9 CFU/ml and diluted to the indicated inoculum in PBS for infection. Mice were anesthetized with Avertin (2,2,2-tribromoethanol dissolved in tert-Amyl alcohol and diluted to a final concentration of 2.5% vol/vol in 0.9% sterile saline) by i.p. injection. For survival experiments, mice were infected with strain Newman at 5 × 10^7 CFU or USA500 at 2.5 × 10^7 CFU by retro-orbital injection. Signs of morbidity (>30% weight loss, ruffled fur, hunched posture, paralysis, inability to walk, or inability to consume food or water) were monitored for 3 wk after infection.

To evaluate bacterial burden in organs, mice were infected with strain Newman at 5 × 10^6 CFU by retro-orbital injection. 4 d or 21 d after infection, sera were collected by submandibular bleeding as described above. Mice were sacrificed, and the indicated organs were weighed, photographed, and/or homogenized to enumerate bacterial burden.

I.p. infections

USA300 strain SF8300 was grown in CCY broth overnight and subcultured in fresh media at 1:100 for 3 h at 37°C with shaking. Bacteria were centrifuged at 4,000 rpm for 10 min and washed two times with 1× PBS. Bacteria were OD normalized to ~10^9 CFU/ml and diluted to the indicated inoculum in PBS for infection. Bacteria were then diluted to ~4 × 10^8 CFU/ml in PBS. Mice were infected by i.p. injection of 200 µl of the diluted bacteria (final inoculum ~8 × 10^7 CFU). Mice were weighed daily after infection; mice that exhibited <5% weight loss after the first day of infection were excluded from the study. 3 dpi, mice were sacrificed, and the indicated organs were homogenized to enumerate bacterial burden.

Serum cytokine measurements

Cytokine concentrations in serum were measured using LEGENDplex multi-analyte flow assay kits for mouse proinflammatory chemokines and mouse Th cytokines (Biolegend). Briefly, standards and samples were diluted at 1:1 with assay buffer, added to the detection beads, and incubated in dark for 2 h at RT with shaking. The beads were washed twice with assay buffer and then incubated with biotinylated detection antibody cocktail in dark for 1 h at RT with shaking. Next, beads were incubated with PE streptavidin for 30 min in dark with shaking. Beads were washed twice and resuspended in assay buffer. Samples were acquired on the Cytoflex instrument. Data were analyzed using the LEGENDplex data analysis software (Biolegend).

To generate the systemic cytokine response heatmap, the averaged concentrations of each cytokine from the indicated groups were normalized by subtracting the mean and dividing by the standard deviation for each cytokine measured (z-score). The order for the rows and columns was determined by unsupervised hierarchical clustering by hclust, R version 3.4.1.

Depletion of CD4 T cells

To deplete CD4 T cells in Swiss Webster mice, the animals were injected i.p. with 100 µg of rat anti-mouse CD4 antibody, clone GK 1.5 (Bio X Cell), or the isotype control antibody rat IgG2b, clone LTF-2 (Bio X Cell), following the depletion scheme depicted in Fig. S4.

The state of CD4 T cell depletion was evaluated by flow cytometry. Blood was collected in heparinized blood collection tubes. 50 µl of blood was washed with 1 ml of PBS at 1,000 *g* for 3 min. Red blood cells were lysed with 1 ml PharmLyse (BD Biosciences) at RT for 5 min. 100 µl of 10× PBS was added immediately and centrifuged at 1,000 *g* for 3 min at RT. Cells were then washed with 1 ml PBS at 1,000 *g* for 3 min, washed once with FACS buffer, and transferred to v-bottom 96-well plates for staining. Cells were incubated with Fc block (anti-mouse CD16/32, clone 24G2; Bio X Cell) in FACS buffer for 10 min on ice. Then, cells were stained with FITC anti-CD3e (eBio500A2; eBioscience), Alexa Fluor 700 anti-CD4 (RM4-5; Biolegend), PerCP Cy 5.5 anti-CD8a (53–6.7; Biolegend), v500 anti-B220 (RA3-6B2; BD Biosciences), and BV605 anti-CD19 (6D5; Biolegend) for 30 min on ice. Cells were washed twice with FACS buffer and fixed with 200 µl of FACS fixing buffer. Cells were strained before sample acquisition on the Cytoflex instrument.

Splenocyte restimulation

Mock- or toxoid-immunized mice were sacrificed 3–5 wk after the last immunization, and the spleens were homogenized to single-cell suspension. For the restimulation, 500,000 splenocytes in RPMI + 10% FBS + 1% penicillin/streptomycin were plated on v-bottom 96-well plates and stimulated with either medium, cell stimulation cocktail (eBioscience), 12.5 µg/ml of the indicated WT leukocidin subunits, or a mixture of 3 µg/ml of $LukE^{mut}$, $LukD^{mut}$, $HlgA^{mut}$, and $HlgB^{mut}$ (toxoids) for 2 d at 37°C with 5% CO_2. Culture supernatants were obtained by centrifuging plates at 4,000 rpm for 10 min at 4°C. Supernatants were stored at −80°C until used. LEGENDplex multi-analyte flow assay kit for mouse Th cytokines was used to measure concentrations of the secreted cytokines as described above. Penicillin/streptomycin was removed from supernantants prior to use by dialysis for the opsonophagocytic killing assays.

Intracellular flow cytometry

Mock- or toxoid-immunized mice were sacrificed 3–5 wk after last immunization. Spleens were homogenized to single-cell suspension. For restimulation, 5 × 10^6 splenocytes in RPMI + 10% FBS + 1% penicillin/streptomycin were plated on 12-well plates and stimulated with media, cell stimulation cocktail (eBioscience), or a mixture of 3 µg/ml of $LukE^{mut}$, $LukD^{mut}$, $HlgA^{mut}$, and $HlgB^{mut}$ (toxoids) overnight at 37°C with 5% CO_2. Protein transport inhibitors (eBioscience) were added to all wells for the last 5 h. Cells were collected in 1.8-ml microcentrifuge tubes, washed once with FACS buffer, and transferred to v-bottom 96-well plates for staining. Cells were incubated with Fc block (anti-mouse CD16/32, clone 24G2; Bio X Cell) in FACS buffer for 10 min on ice. Then, cells were stained with FITC anti-CD3e, AlexaFluor 700 anti-CD4, PerCP Cy 5.5 anti-CD8a, APC anti-CD62L (MEL-14; Biolegend), and PE Cy7 anti-CD44 (IM7; Biolegend) for 30 min on ice. Cells were washed twice with FACS buffer and fixed with 100 µl of FACS fixing buffer for 20 min at RT. Cells were washed with FACS buffer again and permeabilized with permeabilization buffer (0.1% saponin in FACS buffer) for 15 min. Cells were incubated with Fc block in 0.1% saponin for 10 min on ice and stained with

Brilliant Violet 650 anti-IFNγ (XMG1.2; Biolegend) and Brilliant Violet 450 anti-IL17 (TC11-18H10.1; Biolegend) in permeabilization buffer for 30 min. Cells were washed twice with permeabilization buffer and resuspended in FACS buffer. Samples were acquired on the Cytoflex instrument.

Primary mouse BMDMs

Female Swiss Webster mice between 5 and 8 wk old were sacrificed to obtain femurs and tibia. Bone marrow cells were obtained by centrifuging the bones at 10,000 rpm for 2 min on a tabletop centrifuge at RT. Cell pellets were resuspended in 1× PBS and centrifuged at 2,000 rpm for 5 min at RT. Then, cells were washed once with 1× PBS and centrifuged at 2,000 rpm for 5 min at RT. Red blood cells were lysed using 1 ml PharmLyse (BD Biosciences) at RT for 5 min. 10 ml of 1× PBS was added immediately and centrifuged at 2,000 rpm for 10 min at RT. Then, cells were resuspended in 5 ml of 1× PBS, strained using 100-µm cell strainer, and centrifuged at 2,000 rpm for 5 min at RT. Cell pellets were resuspended in RPMI + 10% FBS and counted. To differentiate bone marrow cells from BMDMs, 5×10^6 cells were plated on nontissue culture–treated Petri dishes with BMDM media (Dulbecco's modified Eagle's medium with glutamine and pyruvate, supplemented with 30% L929-conditioned media, 20% FBS, and 50 µM 2-mercaptoethanol) and 1% penicillin/streptomycin for 6 d. On day 6, BMDMs were harvested by treating cells with cold 1× PBS for 30 min.

Opsonophagocytic killing assay

BMDMs were plated at 50,000 cells per well in a flat-bottom tissue culture–treated 96-well plate and cultured in BMDM media overnight. A Newman strain lacking all the β-barrel pore-forming toxins (Δ*lukED* Δ*hlgACB*::*tet* Δ*lukAB*::spec Δ*hla*::ermC; #37.02; VJT) was subcultured at 1:100 in TSB for 3 h. Bacteria were washed with 1× PBS and OD normalized to ~1×10^9 CFU/ml. Bacteria were diluted in RPMI + 10% FBS to 1×10^7 CFU/ml and opsonized with 2% naive mouse serum at 37°C with shaking for 30 min. Cells were stimulated with 10% culture supernatants from the splenocyte restimulations described above in BMDM media or 50 ng (~50–200 U) of recombinant IFNγ and/or recombinant IL17 (Biolegend) in RPMI + 10% FBS for 4 h at 37°C with 5% CO_2. 10 µl of opsonized bacteria was added to all wells and then spun down at 2,000 rpm for 5 min to synchronize the bacteria to the cells. Cells were infected for 1 h at 37°C with 5% CO_2. 11 µl of 10% saponin was added to all wells to lyse the cells for 15 min on ice and then serial diluted to enumerate bacterial survival. Percent bacterial killing = 100 − 100% × (# bacteria after infection/input bacteria).

Graphical and statistical analyses

Analyses of flow cytometric data were performed using FlowJo (Tree Star Software). Statistical significance was determined using Prism 7.0 (GraphPad Software) with the indicated statistical tests.

Online supplemental material

Fig. S1 shows that the concentrations of serum IgG and bacterial burden in the hearts and kidneys are similar for WT- and ΔΔ-infected mice at 35 dpi. Fig. S2 shows that passive immunization protects mice from LukED and HlgAB intoxications. Fig. S3 shows the concentrations of serum cytokine over the course of *S. aureus* i.v. infection. Fig. S4 shows CD4 T cell depletion in toxoid-immunized mice. Fig. S5 shows cytokine production of splenocytes from mock- or toxoid-immunized mice cultured with media, purified leukocidin subunits, or PMA/ionomycin. Table S1 lists the strains used in this study.

Acknowledgments

We thank current and former members of the Torres laboratory for critical insight into this project and helpful comments on the manuscript.

This work was supported in part by the National Institutes of Health (NIH)–National Institute of Allergy and Infectious Diseases award numbers T32AI007180 to K. Tam; R01AI105129, R01AI099394, and HHSN272201400019C to V.J. Torres; and R01AI133977 to P. Loke and V.J. Torres. Work in the S.B. Koralov laboratory was supported by NIH grant no. R01HL125816, a Judith and Stewart Colton Center for Autoimmunity pilot grant, and a grant from the Drs. Martin and Dorothy Spatz Foundation. Flow cytometry technologies were provided by New York University Langone's Cytometry and Cell Sorting Laboratory, which is supported in part by the NIH–National Cancer Institute grant no. P30CA016087. V.J. Torres is a Burroughs Wellcome Fund investigator in the pathogenesis of infectious diseases. V.J. Torres is an inventor on patents and patent applications filed by New York University, which are currently under commercial license to Janssen Biotech Inc. Janssen Biotech Inc. provides research funding and other payments associated with the exclusive licensing agreement.

Author contributions: K. Tam and V.J. Torres conceived and designed experiments with help from S.B. Koralov and P. Loke. K. Tam performed all the vaccination studies with help from K.A. Lacey, A. Sommerfield, R. Chan, and A. O'Malley. M. Coffre and S.B. Koralov provided help with the flow cytometry and intracellular staining. J.C. Devlin and P. Loke provided help with the analysis of the systemic cytokine response. K. Tam and V.J. Torres wrote the manuscript with input from all the other co-authors.

Disclosures: V.J. Torres reported grants from Janssen Biotech Inc. during the conduct of the study outside the submitted work; in addition, V.J. Torres has patents to use leukocidins as *S. aureus* vaccine antigens, which are licensed to Janssen Biotech Inc. No other disclosures were reported.

Submitted: 26 March 2019
Revised: 5 April 2020
Accepted: 8 May 2020

References

Adhikari, R.P., A.O. Ajao, M.J. Aman, H. Karauzum, J. Sarwar, A.D. Lydecker, J.K. Johnson, C. Nguyen, W.H. Chen, and M.C. Roghmann. 2012. Lower Antibody Levels to Staphylococcus Aureus Exotoxins Are Associated With Sepsis in Hospitalized Adults With Invasive S. Aureus Infections. *J. Infect. Dis.* 206:915–923. https://doi.org/10.1093/infdis/jis462

Alonzo, F., III, and V.J. Torres. 2014. The bicomponent pore-forming leucocidins of *Staphylococcus aureus*. *Microbiol. Mol. Biol. Rev.* 78:199–230. https://doi.org/10.1128/MMBR.00055-13

Alonzo, F., III, M.A. Benson, J. Chen, R.P. Novick, B. Shopsin, and V.J. Torres. 2012. *Staphylococcus aureus* leucocidin ED contributes to systemic infection by targeting neutrophils and promoting bacterial growth in vivo. *Mol. Microbiol.* 83:423–435. https://doi.org/10.1111/j.1365-2958.2011.07942.x

Alonzo, F., III, L. Kozhaya, S.A. Rawlings, T. Reyes-Robles, A.L. DuMont, D.G. Myszka, N.R. Landau, D. Unutmaz, and V.J. Torres. 2013. CCR5 is a receptor for *Staphylococcus aureus* leukotoxin ED. *Nature*. 493:51–55. https://doi.org/10.1038/nature11724

Baba, T., T. Bae, O. Schneewind, F. Takeuchi, and K. Hiramatsu. 2008. Genome sequence of *Staphylococcus aureus* strain Newman and comparative analysis of staphylococcal genomes: polymorphism and evolution of two major pathogenicity islands. *J. Bacteriol.* 190:300–310. https://doi.org/10.1128/JB.01000-07

Bagnoli, F., S. Bertholet, and G. Grandi. 2012. Inferring reasons for the failure of *Staphylococcus aureus* vaccines in clinical trials. *Front. Cell. Infect. Microbiol.* 2:16. https://doi.org/10.3389/fcimb.2012.00016

Benson, M.A., E.A. Ohneck, C. Ryan, F. Alonzo, III, H. Smith, A. Narechania, S.O. Kolokotronis, S.W. Satola, A.C. Uhlemann, R. Sebra, et al. 2014. Evolution of hypervirulence by a MRSA clone through acquisition of a transposable element. *Mol. Microbiol.* 93:664–681. https://doi.org/10.1111/mmi.12682

Berends, E.T.M., X. Zheng, E.E. Zwack, M.M. Ménager, M. Cammer, B. Shopsin, and V.J. Torres. 2019. *Staphylococcus aureus* Impairs the Function of and Kills Human Dendritic Cells via the LukAB Toxin. *MBio*. 10. e01918-18. https://doi.org/10.1128/mBio.01918-18

Brown, A.F., A.G. Murphy, S.J. Lalor, J.M. Leech, K.M. O'Keeffe, M. Mac Aogáin, D.P. O'Halloran, K.A. Lacey, M. Tavakol, C.H. Hearnden, et al. 2015. Memory Th1 Cells Are Protective in Invasive *Staphylococcus aureus* Infection. *PLoS Pathog.* 11. e1005226. https://doi.org/10.1371/journal.ppat.1005226

Chambers, H.F., and F.R. Deleo. 2009. Waves of resistance: *Staphylococcus aureus* in the antibiotic era. *Nat. Rev. Microbiol.* 7:629–641. https://doi.org/10.1038/nrmicro2200

Chan, R., P.T. Buckley, A. O'Malley, W.E. Sause, F. Alonzo, III, A. Lubkin, K.M. Boguslawski, A. Payne, J. Fernandez, W.R. Strohl, et al. 2019. Identification of biologic agents to neutralize the bicomponent leukocidins of *Staphylococcus aureus*. *Sci. Transl. Med.* 11. eaat0882. https://doi.org/10.1126/scitranslmed.aat0882

Chang, F.Y., J.E. Peacock, Jr., D.M. Musher, P. Triplett, B.B. MacDonald, J.M. Mylotte, A. O'Donnell, M.M. Wagener, and V.L. Yu. 2003. *Staphylococcus aureus* bacteremia: recurrence and the impact of antibiotic treatment in a prospective multicenter study. *Medicine (Baltimore)*. 82:333–339. https://doi.org/10.1097/01.md.0000091184.93122.09

Chapman, J.R., D. Balasubramanian, K. Tam, M. Askenazi, R. Copin, B. Shopsin, V.J. Torres, and B.M. Ueberheide. 2017. Using Quantitative Spectrometry to Understand the Influence of Genetics and Nutritional Perturbations On the Virulence Potential of *Staphylococcus aureus*. *Mol. Cell. Proteomics*. 16(4, suppl 1):S15–S28. https://doi.org/10.1074/mcp.O116.065581

Cho, J.S., E.M. Pietras, N.C. Garcia, R.I. Ramos, D.M. Farzam, H.R. Monroe, J.E. Magorien, A. Blauvelt, J.K. Kolls, A.L. Cheung, et al. 2010. IL-17 is essential for host defense against cutaneous *Staphylococcus aureus* infection in mice. *J. Clin. Invest.* 120:1762–1773. https://doi.org/10.1172/JCI40891

ClinicalTrials.gov. 2019. Prevention of S. aureus Pneumonia Study in Mechanically Ventilated Subjects Who Are Heavily Colonized With S. Aureus. https://clinicaltrials.gov/ct2/show/NCT02940626

Creech, C.B., D.N. Al-Zubeidi, and S.A. Fritz. 2015. Prevention of Recurrent Staphylococcal Skin Infections. *Infect. Dis. Clin. North Am.* 29:429–464. https://doi.org/10.1016/j.idc.2015.05.007

DuMont, A.L., T.K. Nygaard, R.L. Watkins, A. Smith, L. Kozhaya, B.N. Kreiswirth, B. Shopsin, D. Unutmaz, J.M. Voyich, and V.J. Torres. 2011. Characterization of a new cytotoxin that contributes to *Staphylococcus aureus* pathogenesis. *Mol. Microbiol.* 79:814–825. https://doi.org/10.1111/j.1365-2958.2010.07490.x

DuMont, A.L., P. Yoong, C.J. Day, F. Alonzo, III, W.H. McDonald, M.P. Jennings, and V.J. Torres. 2013. *Staphylococcus aureus* LukAB cytotoxin kills human neutrophils by targeting the CD11b subunit of the integrin Mac-1. *Proc. Natl. Acad. Sci. USA*. 110:10794–10799. https://doi.org/10.1073/pnas.1305121110

Dunman, P.M., E. Murphy, S. Haney, D. Palacios, G. Tucker-Kellogg, S. Wu, E.L. Brown, R.J. Zagursky, D. Shlaes, and S.J. Projan. 2001. Transcription profiling-based identification of *Staphylococcus aureus* genes regulated by the agr and/or sarA loci. *J. Bacteriol.* 183:7341–7353. https://doi.org/10.1128/JB.183.24.7341-7353.2001

Duthie, E.S., and L.L. Lorenz. 1952. Staphylococcal coagulase; mode of action and antigenicity. *J. Gen. Microbiol.* 6:95–107.

Ellis, T.N., and B.L. Beaman. 2004. Interferon-gamma activation of polymorphonuclear neutrophil function. *Immunology*. 112:2–12. https://doi.org/10.1111/j.1365-2567.2004.01849.x

Foster, T.J.. 2005. Immune evasion by staphylococci. *Nat. Rev. Microbiol.* 3:948–958. https://doi.org/10.1038/nrmicro1289

Giersing, B.K., S.S. Dastgheyb, K. Modjarrad, and V. Moorthy. 2016. Status of vaccine research and development of vaccines for *Staphylococcus aureus*. *Vaccine*. 34:2962–2966. https://doi.org/10.1016/j.vaccine.2016.03.110

Gold, H.S., and S.K. Pillai. 2009. Antistaphylococcal agents. *Infect. Dis. Clin. North Am.* 23:99–131. https://doi.org/10.1016/j.idc.2008.10.008

Goodyear, C.S., and G.J. Silverman. 2003. Death by a B cell superantigen: In vivo VH-targeted apoptotic supraclonal B cell deletion by a Staphylococcal Toxin. *J. Exp. Med.* 197:1125–1139. https://doi.org/10.1084/jem.20020552

Hermos, C.R., P. Yoong, and G.B. Pier. 2010. High levels of antibody to panton-valentine leukocidin are not associated with resistance to *Staphylococcus aureus*-associated skin and soft-tissue infection. *Clin. Infect. Dis.* 51:1138–1146. https://doi.org/10.1086/656742

Ishigame, H., S. Kakuta, T. Nagai, M. Kadoki, A. Nambu, Y. Komiyama, N. Fujikado, Y. Tanahashi, A. Akitsu, H. Kotaki, et al. 2009. Differential roles of interleukin-17A and -17F in host defense against mucoepithelial bacterial infection and allergic responses. *Immunity*. 30:108–119. https://doi.org/10.1016/j.immuni.2008.11.009

Keener, A.B., L.T. Thurlow, S. Kang, N.A. Spidale, S.H. Clarke, K.M. Cunnion, R. Tisch, A.R. Richardson, and B.J. Vilen. 2017. *Staphylococcus aureus* Protein A Disrupts Immunity Mediated by Long-Lived Plasma Cells. *J. Immunol.* 198:1263–1273. https://doi.org/10.4049/jimmunol.1600093

Kennedy, A.D., J. Bubeck Wardenburg, D.J. Gardner, D. Long, A.R. Whitney, K.R. Braughton, O. Schneewind, and F.R. DeLeo. 2010. Targeting of alpha-hemolysin by active or passive immunization decreases severity of USA300 skin infection in a mouse model. *J. Infect. Dis.* 202:1050–1058. https://doi.org/10.1086/656043

Kim, H.K., A.G. Cheng, H.Y. Kim, D.M. Missiakas, and O. Schneewind. 2010. Nontoxigenic protein A vaccine for methicillin-resistant *Staphylococcus aureus* infections in mice. *J. Exp. Med.* 207:1863–1870. https://doi.org/10.1084/jem.20092514

Lacey, K.A., J.M. Leech, S.J. Lalor, N. McCormack, J.A. Geoghegan, and R.M. McLoughlin. 2017. The *Staphylococcus aureus* Cell Wall-Anchored Protein Clumping Factor A Is an Important T Cell Antigen. *Infect. Immun.* 85. e00549-17. https://doi.org/10.1128/IAI.00549-17

Lee, B., R. Olaniyi, J.M. Kwiecinski, and J.B. Wardenburg. 2020. Staphylococcus aureus toxin suppresses antigen-specific T cell responses. *J. Clin. Invest.* 130:1122–1127. https://doi.org/10.1172/JCI130728

Lin, L., A.S. Ibrahim, X. Xu, J.M. Farber, V. Avanesian, B. Baquir, Y. Fu, S.W. French, J.E. Edwards, Jr., and B. Spellberg. 2009. Th1-Th17 cells mediate protective adaptive immunity against *Staphylococcus aureus* and Candida albicans infection in mice. *PLoS Pathog.* 5. e1000703. https://doi.org/10.1371/journal.ppat.1000703

Lubkin, A., W.L. Lee, F. Alonzo, III, C. Wang, J. Aligo, M. Keller, N.M. Girgis, T. Reyes-Robles, R. Chan, A. O'Malley, et al. 2019. *Staphylococcus aureus* Leukocidins Target Endothelial DARC to Cause Lethality in Mice. *Cell Host Microbe*. 25:463–470.e9. https://doi.org/10.1016/j.chom.2019.01.015

Miller, L.S., and J.S. Cho. 2011. Immunity against *Staphylococcus aureus* cutaneous infections. *Nat. Rev. Immunol.* 11:505–518. https://doi.org/10.1038/nri3010

Miller, L.G., C. Quan, A. Shay, K. Mostafaie, K. Bharadwa, N. Tan, K. Matayoshi, J. Cronin, J. Tan, G. Tagudar, et al. 2007. A prospective investigation of outcomes after hospital discharge for endemic, community-acquired methicillin-resistant and -susceptible *Staphylococcus aureus* skin infection. *Clin. Infect. Dis.* 44:483–492. https://doi.org/10.1086/511041

Monaci, E., F. Mancini, G. Lofano, M. Bacconi, S. Tavarini, C. Sammicheli, L. Arcidiacono, M. Giraldi, B. Galletti, S. Rossi Paccani, et al. 2015. MF59- and Al(OH)3-Adjuvanted *Staphylococcus aureus* (4C-Staph) Vaccines Induce Sustained Protective Humoral and Cellular Immune Responses, with a Critical Role for Effector CD4 T Cells at Low Antibody Titers. *Front. Immunol.* 6:439. https://doi.org/10.3389/fimmu.2015.00439

Montgomery, C.P., S. Boyle-Vavra, and R.S. Daum. 2009. The arginine catabolic mobile element is not associated with enhanced virulence in experimental invasive disease caused by the community-associated methicillin-resistant *Staphylococcus aureus* USA300 genetic background. *Infect. Immun.* 77:2650–2656. https://doi.org/10.1128/IAI.00256-09

Montgomery, C.P., M. Daniels, F. Zhao, M.L. Alegre, A.S. Chong, and R.S. Daum. 2014. Protective immunity against recurrent *Staphylococcus*

aureus skin infection requires antibody and interleukin-17A. *Infect. Immun.* 82:2125–2134. https://doi.org/10.1128/IAI.01491-14

Nakai, K., Y.Y. He, F. Nishiyama, F. Naruse, R. Haba, Y. Kushida, N. Katsuki, T. Moriue, K. Yoneda, and Y. Kubota. 2017. IL-17A induces heterogeneous macrophages, and it does not alter the effects of lipopolysaccharides on macrophage activation in the skin of mice. *Sci. Rep.* 7:12473. https://doi.org/10.1038/s41598-017-12756-y

Narita, K., D.L. Hu, F. Mori, K. Wakabayashi, Y. Iwakura, and A. Nakane. 2010. Role of interleukin-17A in cell-mediated protection against *Staphylococcus aureus* infection in mice immunized with the fibrinogen-binding domain of clumping factor A. *Infect. Immun.* 78:4234–4242. https://doi.org/10.1128/IAI.00447-10

Nathan, C.F., H.W. Murray, M.E. Wiebe, and B.Y. Rubin. 1983. Identification of interferon-gamma as the lymphokine that activates human macrophage oxidative metabolism and antimicrobial activity. *J. Exp. Med.* 158: 670–689. https://doi.org/10.1084/jem.158.3.670

Pauli, N.T., H.K. Kim, F. Falugi, M. Huang, J. Dulac, C. Henry Dunand, N.Y. Zheng, K. Kaur, S.F. Andrews, Y. Huang, et al. 2014. *Staphylococcus aureus* infection induces protein A-mediated immune evasion in humans. *J. Exp. Med.* 211:2331–2339. https://doi.org/10.1084/jem.20141404

Pelzek, A.J., B. Shopsin, E.E. Radke, K. Tam, B.M. Ueberheide, D. Fenyö, S.M. Brown, Q. Li, A. Rubin, Y. Fulmer, et al. 2018. Human Memory B Cells Targeting *Staphylococcus aureus* Exotoxins Are Prevalent with Skin and Soft Tissue Infection. *MBio.* 9. e02125-17. https://doi.org/10.1128/mBio.02125-17

Pishchany, G., S.E. Dickey, and E.P. Skaar. 2009. Subcellular localization of the *Staphylococcus aureus* heme iron transport components IsdA and IsdB. *Infect. Immun.* 77:2624–2634. https://doi.org/10.1128/IAI.01531-08

Radke, E.E., S.M. Brown, A.J. Pelzek, Y. Fulmer, D.N. Hernandez, V.J. Torres, I.P. Thomsen, W.K. Chiang, A.O. Miller, B. Shopsin, et al. 2018. Hierarchy of human IgG recognition within the *Staphylococcus aureus* immunome. *Sci. Rep.* 8:13296. https://doi.org/10.1038/s41598-018-31424-3

Reyes-Robles, T., F. Alonzo, III, L. Kozhaya, D.B. Lacy, D. Unutmaz, and V.J. Torres. 2013. *Staphylococcus aureus* leukotoxin ED targets the chemokine receptors CXCR1 and CXCR2 to kill leukocytes and promote infection. *Cell Host Microbe.* 14:453–459. https://doi.org/10.1016/j.chom.2013.09.005

Reyes-Robles, T., A. Lubkin, F. Alonzo, III, D.B. Lacy, and V.J. Torres. 2016. Exploiting dominant-negative toxins to combat *Staphylococcus aureus* pathogenesis. *EMBO Rep.* 17:428–440. https://doi.org/10.15252/embr.201540994

Romagnani, S., M.G. Giudizi, G. del Prete, E. Maggi, R. Biagiotti, F. Almerigogna, and M. Ricci. 1982. Demonstration on protein A of two distinct immunoglobulin-binding sites and their role in the mitogenic activity of *Staphylococcus aureus* Cowan I on human B cells. *J. Immunol.* 129:596–602.

Salgado-Pabón, W., and P.M. Schlievert. 2014. Models matter: the search for an effective *Staphylococcus aureus* vaccine. *Nat. Rev. Microbiol.* 12: 585–591. https://doi.org/10.1038/nrmicro3308

Septimus, E.J., and M.L. Schweizer. 2016. Decolonization in Prevention of Health Care-Associated Infections. *Clin. Microbiol. Rev.* 29:201–222. https://doi.org/10.1128/CMR.00049-15

Seybold, U., E.V. Kourbatova, J.G. Johnson, S.J. Halvosa, Y.F. Wang, M.D. King, S.M. Ray, and H.M. Blumberg. 2006. Emergence of community-associated methicillin-resistant *Staphylococcus aureus* USA300 genotype as a major cause of health care-associated blood stream infections. *Clin. Infect. Dis.* 42:647–656. https://doi.org/10.1086/499815

Spaan, A.N., T. Henry, W.J.M. van Rooijen, M. Perret, C. Badiou, P.C. Aerts, J. Kemmink, C.J.C. de Haas, K.P.M. van Kessel, F. Vandenesch, et al. 2013. The staphylococcal toxin Panton-Valentine Leukocidin targets human C5a receptors. *Cell Host Microbe.* 13:584–594. https://doi.org/10.1016/j.chom.2013.04.006

Spaan, A.N., M. Vrieling, P. Wallet, C. Badiou, T. Reyes-Robles, E.A. Ohneck, Y. Benito, C.J. de Haas, C.J. Day, M.P. Jennings, et al. 2014. The staphylococcal toxins γ-haemolysin AB and CB differentially target phagocytes by employing specific chemokine receptors. *Nat. Commun.* 5: 5438. https://doi.org/10.1038/ncomms6438

Spaan, A.N., T. Reyes-Robles, C. Badiou, S. Cochet, K.M. Boguslawski, P. Yoong, C.J. Day, C.J. de Haas, K.P. van Kessel, F. Vandenesch, et al. 2015. *Staphylococcus aureus* Targets the Duffy Antigen Receptor for Chemokines (DARC) to Lyse Erythrocytes. *Cell Host Microbe.* 18:363–370. https://doi.org/10.1016/j.chom.2015.08.001

Spaan, A.N., J.A.G. van Strijp, and V.J. Torres. 2017. Leukocidins: staphylococcal bi-component pore-forming toxins find their receptors. *Nat. Rev. Microbiol.* 15:435–447. https://doi.org/10.1038/nrmicro.2017.27

Thammavongsa, V., H.K. Kim, D. Missiakas, and O. Schneewind. 2015. Staphylococcal manipulation of host immune responses. *Nat. Rev. Microbiol.* 13:529–543. https://doi.org/10.1038/nrmicro3521

Thomsen, I.P., A.L. Dumont, D.B. James, P. Yoong, B.R. Saville, N. Soper, V.J. Torres, and C.B. Creech. 2014. Children with invasive *Staphylococcus aureus* disease exhibit a potently neutralizing antibody response to the cytotoxin LukAB. *Infect. Immun.* 82:1234–1242. https://doi.org/10.1128/IAI.01558-13

Tong, S.Y., J.S. Davis, E. Eichenberger, T.L. Holland, and V.G. Fowler, Jr.. 2015. *Staphylococcus aureus* infections: epidemiology, pathophysiology, clinical manifestations, and management. *Clin. Microbiol. Rev.* 28:603–661. https://doi.org/10.1128/CMR.00134-14

van Hal, S.J., S.O. Jensen, V.L. Vaska, B.A. Espedido, D.L. Paterson, and I.B. Gosbell. 2012. Predictors of mortality in *Staphylococcus aureus* Bacteremia. *Clin. Microbiol. Rev.* 25:362–386. https://doi.org/10.1128/CMR.05022-11

Wertheim, H.F., D.C. Melles, M.C. Vos, W. van Leeuwen, A. van Belkum, H.A. Verbrugh, and J.L. Nouwen. 2005. The role of nasal carriage in *Staphylococcus aureus* infections. *Lancet Infect. Dis.* 5:751–762. https://doi.org/10.1016/S1473-3099(05)70295-4

Wilke, G.A., and J. Bubeck Wardenburg. 2010. Role of a disintegrin and metalloprotease 10 in *Staphylococcus aureus* α-hemolysin-mediated cellular injury. *Proc. Natl. Acad. Sci. USA.* 107:13473–13478. https://doi.org/10.1073/pnas.1001815107

Yoong, P., and V.J. Torres. 2013. The effects of Staphylococcus aureus leukotoxins on the host: cell lysis and beyond. *Curr. Opin. Microbiol.* 16: 63–69. https://doi.org/10.1016/j.mib.2013.01.012

Zhang, L., K. Jacobsson, J. Vasi, M. Lindberg, and L. Frykberg. 1998. A second IgG-binding protein in *Staphylococcus aureus*. *Microbiology.* 144:985–991. https://doi.org/10.1099/00221287-144-4-985

Zhao, Y.X., I.M. Nilsson, and A. Tarkowski. 1998. The dual role of interferon-gamma in experimental Staphylococcus aureus septicaemia versus arthritis. *Immunology.* 93:80–85. https://doi.org/10.1046/j.1365-2567.1998.00407.x

Zhao, F., B.L. Cheng, S. Boyle-Vavra, M.L. Alegre, R.S. Daum, A.S. Chong, and C.P. Montgomery. 2015. Proteomic Identification of saeRS-Dependent Targets Critical for Protective Humoral Immunity against *Staphylococcus aureus* Skin Infection. *Infect. Immun.* 83:3712–3721. https://doi.org/10.1128/IAI.00667-15

Supplemental material

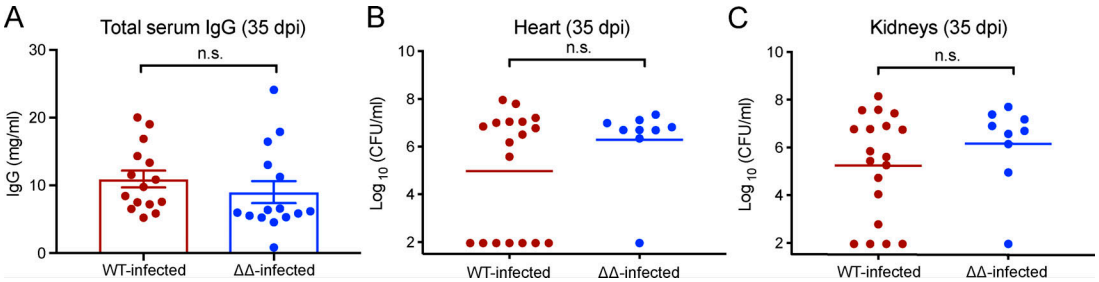

Figure S1. **Serum IgG and bacterial burden are similar for WT- and ΔΔ-infected mice at 35 dpi. (A)** Bar graph depicts the averaged concentration of total serum IgG in WT-infected and ΔΔ-infected mice at 35 dpi ± SEM. Statistical analyses were performed with unpaired Student's *t* test. (**B and C)** Bacterial burdens in hearts (B) and kidneys (C) were enumerated on 35 dpi. Graphs depict the averaged bacterial burden of the indicated organ. Statistical analyses were performed with Mann-Whitney tests. Circles indicate IgG concentration or bacterial burden of individual mice. *n* = 9–15 mice per group. n.s., not significant.

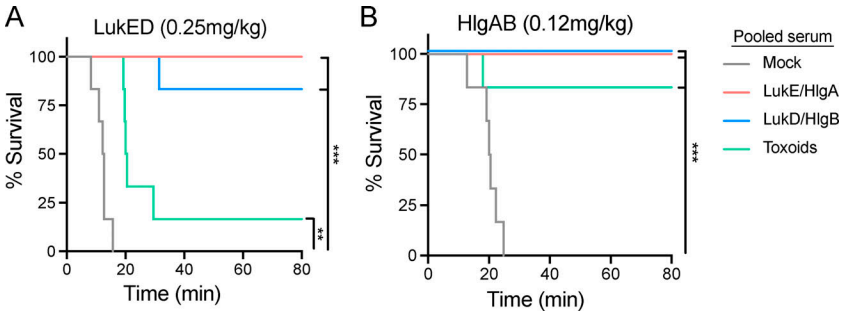

Figure S2. **Passive immunization protects mice from LukED and HlgAB intoxications. (A and B)** Naive mice were passive immunized with pooled serum isolated from mock-immunized or the indicated leukocidin-immunized mice ~24 h before intoxication with purified LukED (A) or HlgAB (B). Morbidity of the animals was monitored for 80 min. Statistical analyses were performed with log-rank (Mantel-Cox) test corrected for multiple comparisons. *n* = 6 mice per group. **, P < 0.01; ***, P < 0.001.

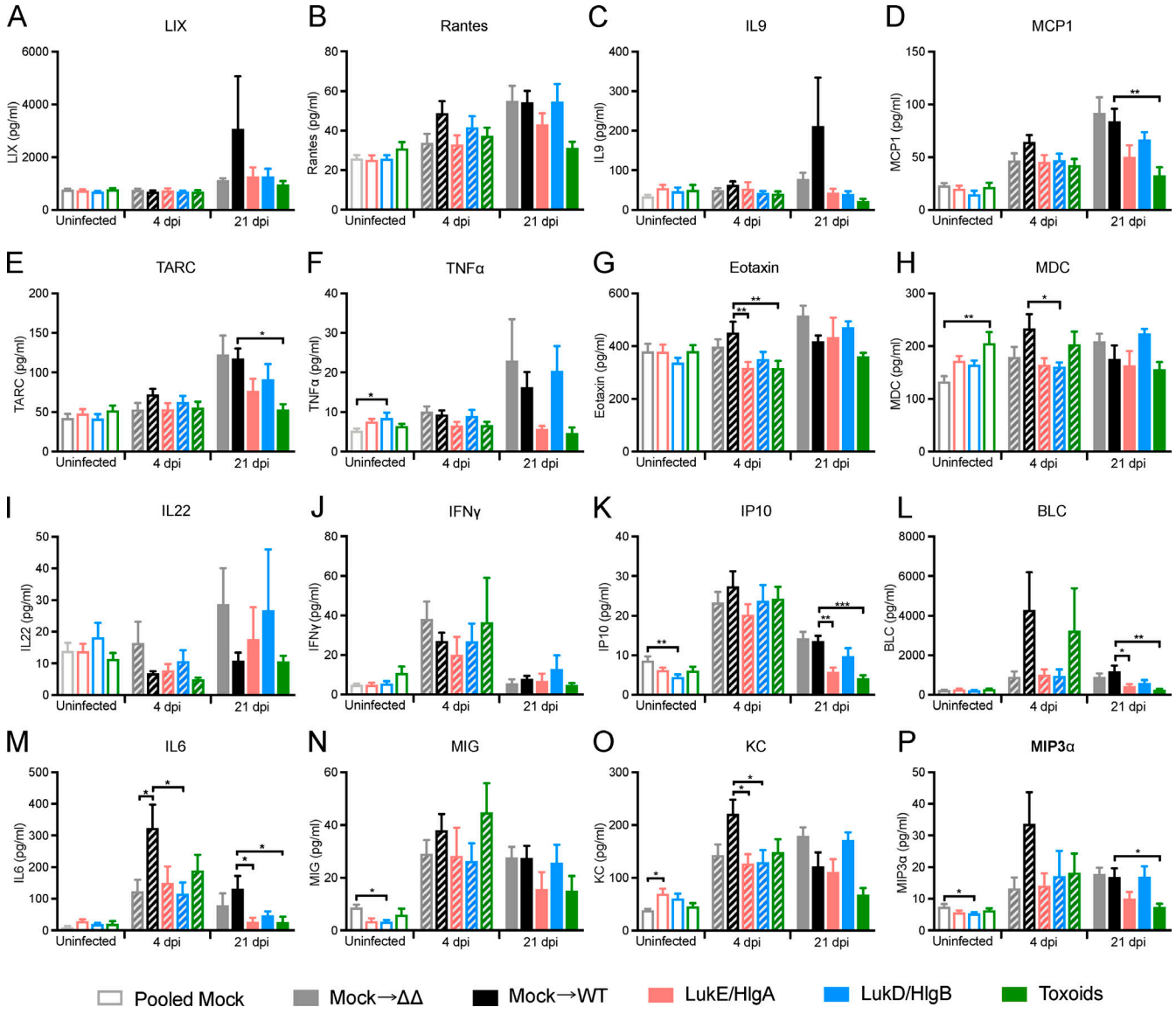

Figure S3. **Concentrations of serum cytokine over the course of *S. aureus* IV infection. (A–P)** Raw data for Fig. 4. Serum concentrations of the indicated cytokines were measured over the course of infection. Bar graphs depict the averaged concentration + SEM of the following cytokines: LIX (A), Rantes (B), IL9 (C), MCP1 (D), TARC (E), TNFα (F), Eotaxin (G), MDC (H), IL22 (I), IFNγ (J), IP10 (K), BLC (L), IL6 (M), MIG (N), KC (O), and MIP3α (P). Statistical analyses were performed with one-way ANOVA, corrected with Dunnett's multiple comparison, comparing against mock for the uninfected group or against mock infected with WT *S. aureus* for the 4 dpi and 21 dpi groups. n = 20 mice per group for uninfected mice, 15 mice per group for 4 dpi, and 4 or 5 mice per group for 21 dpi. *, P = 0.05; **, P < 0.01; ***, P < 0.001.

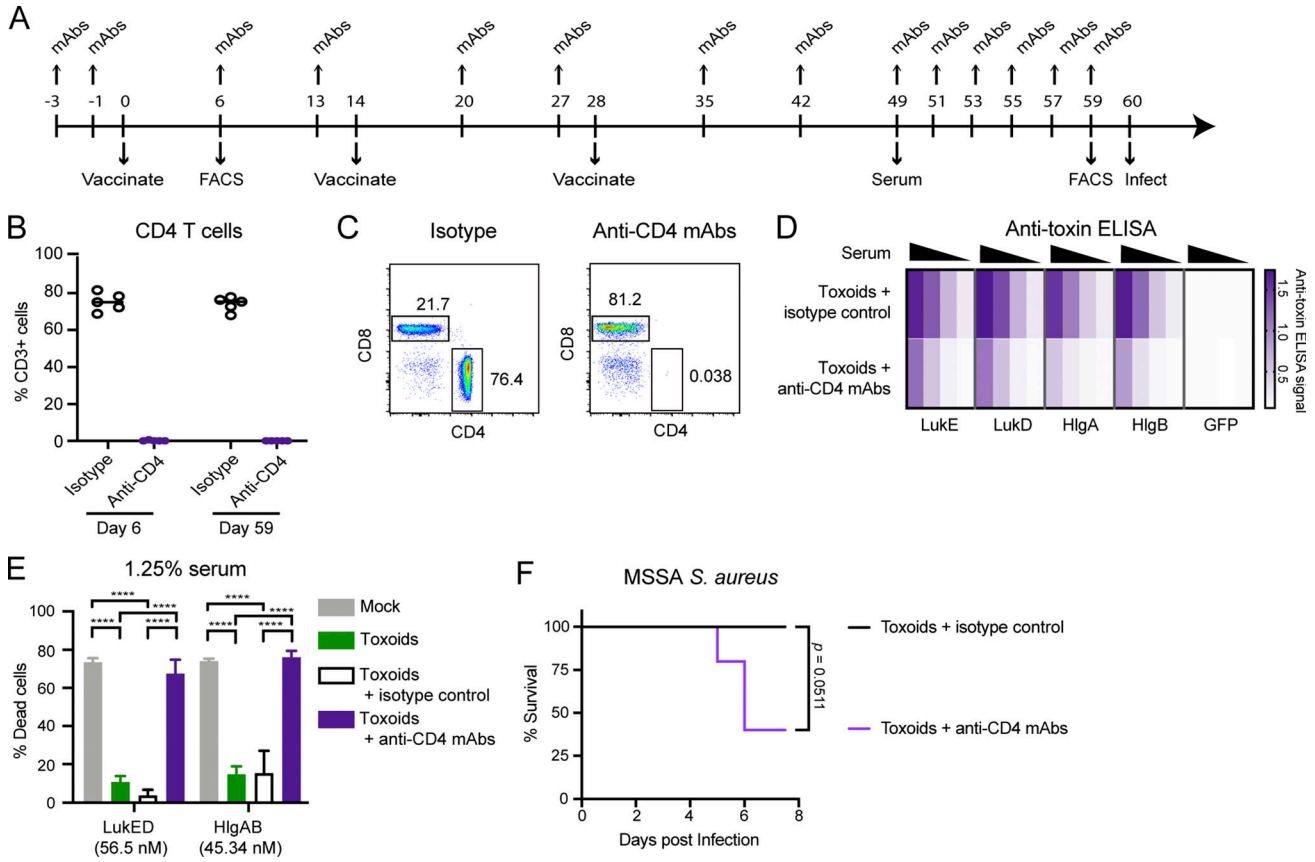

Figure S4. **CD4 T cell depletion in toxoid-immunized mice. (A)** Experimental scheme for the CD4 T cell depletion study. **(B)** CD4 T cells present in the blood of toxoid-immunized mice treated with isotype control or CD4-depletion antibodies on day 6 after immunization and day 59 after immunization. *n* = 5 mice per group. Circles represent individual mice. **(C)** Representative flow cytometry plots depicting the depletion status of CD4 T cells in isotype-treated (left) and anti-CD4 mAbs-treated (right) mice on day 59. **(D)** Heatmap representing the titer of serum antibodies against the indicated leukocidin isolated from toxoid-immunized mice treated with isotype control or CD4-depletion antibodies. *n* = 5 mice per group. **(E)** Neutralization activity of serum antibodies isolated from mock-immunized mice, toxoid-immunized mice, and toxoid-immunized mice treated with isotype control or CD4-depletion antibodies on hPMNs intoxicated with LukED or HlgAB. Cell viability was determined by the metabolic dye CellTiter. Bar graph depicts the averaged percent killing of hPMN + SEM. Statistical analysis was performed with two-way ANOVA, corrected with Dunnett's multiple comparison. *n* = 5 mice and 2 hPMN donors per group. ****, $P < 0.0001$. **(F)** Survival of toxoid-immunized mice treated with isotype control mAbs or anti–CD4-depletion mAbs upon retro-orbital infection with 5×10^7 WT *S. aureus* strain Newman. Morbidity of the animals was monitored for 7 d. *n* = 5 mice per group. Statistical analysis was performed with log-rank (Mantel-Cox) test.

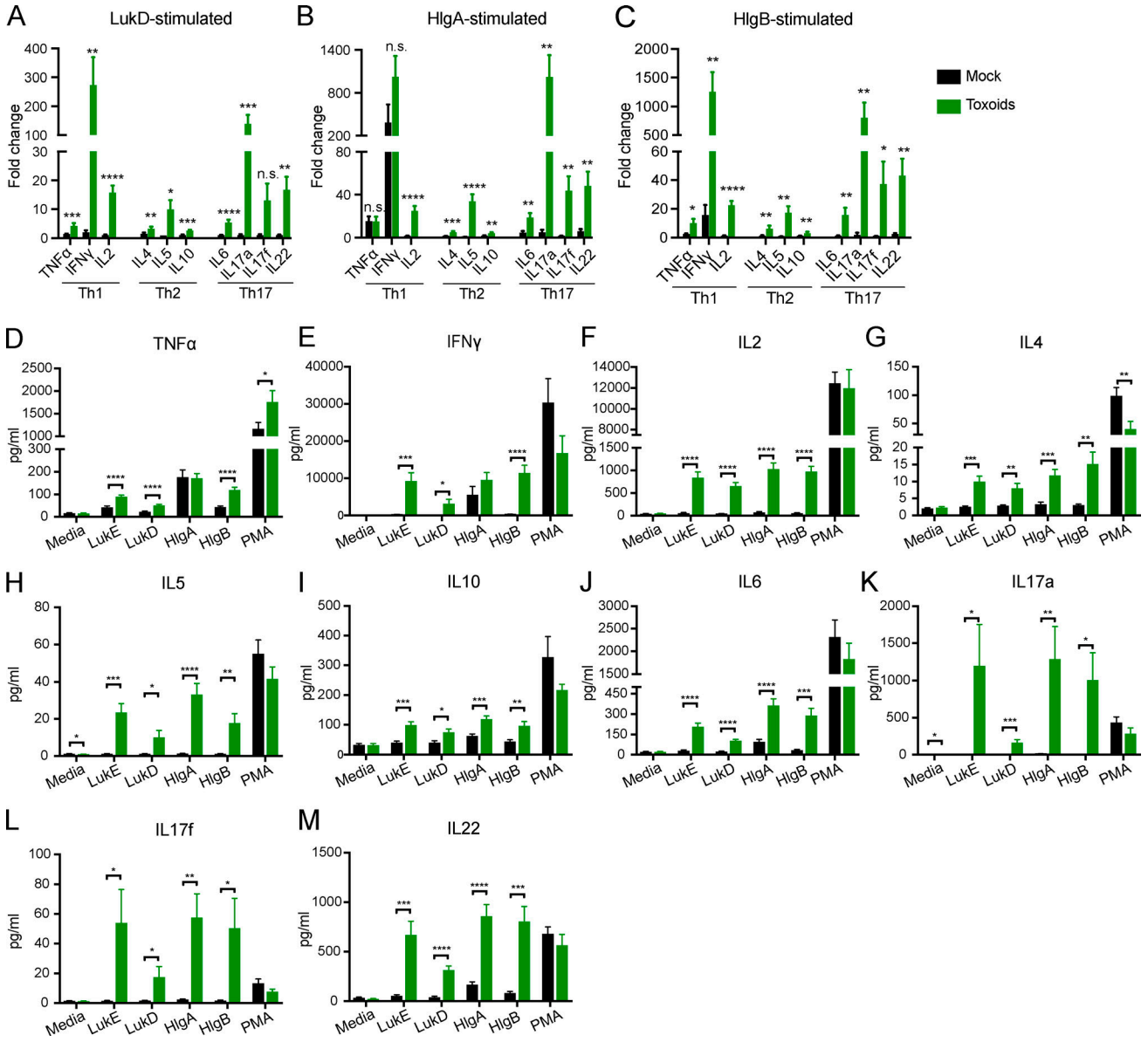

Figure S5. **Cytokine production of splenocytes from mock- or toxoid-immunized mice cultured with media, purified leukocidin subunits, or PMA/ionomycin. (A–C)** Splenocytes from mock- or toxoid-immunized mice were cultured with media and LukD (A), HlgA (B), or HlgB (C). Culture supernatants were collected to measure the concentrations of secreted cytokines. Bar graph depicts averaged fold change of the indicated leukocidin-stimulated splenocytes over media-treated controls for the indicated cytokine + SEM. Statistical analyses were performed with unpaired Student's *t* test between the splenocytes from mock- and toxoid-immunized mice for each cytokine. **(D–M)** Raw data for Fig. 5, B and C; and Fig. S4, A and B. Concentrations of the indicated cytokines in the culture supernatants of mock- or toxoid-immunized splenocytes cultured with media only, the indicated leukocidins, or PMA/ionomycin were measured by LEGENDplex multi-analyte flow assay kits. Bar graphs depict the averaged concentration + SEM of the following cytokines: TNFα (D), IFNγ (E), IL2 (F), IL4 (G), IL5 (H), IL10 (I), IL6 (J), IL17a (K), IL17f (L), and IL22 (M). Statistical analyses were performed with unpaired Student's *t* test between the splenocytes from mock- and toxoid-immunized mice for matched treatment conditions. n = 10 mice. *, P = 0.05; **, P < 0.01; ***, P < 0.001; ****, P < 0.0001. n.s., not significant.

Table S1 is provided online as a separate Word document and lists the strains used in this study.